Reviewer 1

The manuscript analyses streamflow trends in 38 Chilean catchments over the 2001–2021 period and examines their correlations with precipitation, air temperature, and soil moisture. Mann-Kendall and Theil-Sen trend analyses are applied to in situ streamflow records, a local gridded precipitation dataset (CR2MET), and the GLDAS-Noah reanalysis soil moisture product (rather than the SMAP/SMOS satellite datasets mentioned in the abstract).

However, the manuscript is poorly structured and difficult to follow. Several statements are not supported by quantitative results derived from the analysis. Moreover, the study lacks a clearly articulated scientific question or testable hypothesis. Although three specific objectives are stated, two of them are not fully addressed in the Results and Discussion sections. The datasets and methodological approaches employed are standard and do not present methodological innovation. In addition, the maps shown in the Results section do not depict spatially continuous hydrological variables and would be more appropriately represented using coloured symbols. Some of the conclusions are speculative and not sufficiently supported by the evidence provided.

In its current form, the manuscript does not constitute a substantial contribution to the hydrological literature. The major and minor issues identified are detailed below.

R. We sincerely thank the reviewer for the thorough, constructive, and insightful evaluation of our manuscript. We greatly appreciate the time and expertise invested in the review process. The comments have been extremely valuable and have guided a substantial revision of the manuscript, leading to important improvements in its clarity, methodological consistency, and overall scientific contribution.

We acknowledge that the original version of the manuscript did not sufficiently articulate its conceptual framework, and that several aspects of the structure, methodology, and interpretation required clarification and refinement. In response, we have carefully revised the manuscript to address all major and minor comments transparently and systematically.

First, the study's conceptual framing has been strengthened. The Introduction has been fully rewritten to clearly define the scientific context, explicitly present the conceptual links between hydroclimatic variables and peak streamflow generation, and formulate consistent, well-aligned objectives. The scope of the study is now more clearly defined as an analysis of statistical associations, avoiding any unintended causal interpretation.

Second, the methodological approach has been refined to improve physical consistency. We have implemented an event-based annual framework, in which hydroclimatic variables are evaluated at the timing of annual maximum streamflow and over antecedent periods. This revision ensures temporal alignment between variables and provides a more physically coherent basis for interpreting hydroclimatic conditions associated with peak flows.

Third, the Results and Discussion sections have been thoroughly revised. Variable definitions and climate classifications have been standardized throughout the manuscript, and all interpretative statements are now explicitly supported by the corresponding analyses and figures. Statements that were previously speculative or beyond the scope of the methodology have been removed or carefully reformulated. In addition, spatial patterns are now more explicitly analyzed and discussed, improving the interpretability of the results.

Fourth, the presentation of results has been improved following the reviewer's suggestions. The original maps have been redesigned into consolidated national-scale figures using symbol-based representations, which better reflect the catchment-based nature of the data and facilitate comparison across variables.

Finally, we have clarified the scope and contribution of the study. While the methods employed are well established, the revised manuscript now more clearly presents its contribution as a consistent, multivariable, and spatially comparative assessment of hydroclimatic conditions associated with peak streamflow across contrasting climatic regimes in Chile. The study is intended as an exploratory, comparative analysis that provides insight into regional hydroclimatic variability and its association with extreme streamflow behavior.

We have carefully addressed all comments raised by the reviewer, and detailed, point-by-point responses are provided below. We are grateful for the reviewer's feedback, which has significantly strengthened the manuscript, and we hope the revised version meets the reviewer's and the journal's expectations.

Major comments:

- **MC1. The motivation of the manuscript is insufficiently developed**. The Introduction reviews several studies from Chile and other regions documenting increases in air temperature, decreases in precipitation and streamflow, and the growing attention given to soil moisture as a potential explanatory variable of streamflow trends. However, it does not provide a clear conceptual framework describing the relationship between hydroclimatic drivers and streamflow patterns, as suggested by the title. Furthermore, the Introduction does not clearly state whether the study aims to identify spatial,

> temporal, or spatio-temporal streamflow patterns. It also lacks a strong justification for the three stated objectives: (i) quantifying trends in annual maximum streamflows; (ii) identifying dominant hydroclimatic controls on streamflow; and (iii) assessing regional variations in climate–streamflow relationships. The importance and novelty of addressing these objectives are not sufficiently articulated.

R. We thank the reviewer for this comment. We agree that the original Introduction did not clearly articulate the conceptual framework linking hydroclimatic variables to streamflow responses, nor did it sufficiently clarify the study's scope and scientific motivation.

In the revised manuscript, the Introduction has been substantially rewritten to improve its structure and to clarify the study rationale. The revised version now explicitly:
(i) Presents the conceptual framework linking precipitation, temperature, and antecedent soil moisture with peak streamflow generation.
(ii) Clarifies that the study focuses on temporal trends in annual maximum streamflow and examines hydroclimatic conditions associated with peak flows.
(iii) Better articulates the scientific motivation and relevance of the three study objectives.

In addition, the objectives have been reformulated to avoid causal interpretations and to emphasize that the analysis focuses on statistical associations between peak streamflow and hydroclimatic conditions across contrasting climate regimes.

The revised introduction is included below and constitutes the new “1. Introduction” section in the manuscript.

Revised Introduction:

“Climate change is altering hydrological systems worldwide by modifying precipitation regimes, temperature patterns, and the frequency and magnitude of hydrological extremes (IPCC, 2023; Blöschl et al., 2019; Costa et al., 2023; Qiu et al., 2023; Sukanya and Joseph, 2023). In this context, understanding the occurrence of high streamflow events is essential for flood risk assessment, water resources management, and ecosystem functioning. Hydroclimatic conditions, including precipitation, temperature, and antecedent soil moisture, influence peak streamflow events. Understanding how these factors affect the occurrence and variability of peak flows is therefore essential for interpreting hydrological extremes across different climatic settings.

Peak streamflow events are typically generated by the interaction of multiple hydroclimatic factors, including precipitation intensity and accumulation, antecedent soil moisture conditions, and temperature dependent processes such as evapotranspiration or snowmelt. Previous studies have shown that precipitation is often the primary driver of high flows, while soil moisture can strongly modulate runoff responses by controlling catchment storage and infiltration capacity (Wasko and Nathan, 2019; Alam et al., 2024). Temperature also plays an important role in regulating hydrological processes through its influence on evapotranspiration, snow accumulation and melt dynamics, and the partitioning of precipitation between rainfall and snowfall. Because these variables interact in complex ways, multivariable approaches are increasingly used to analyze hydroclimatic variability and its relationship with streamflow extremes (Swain et al., 2024).

At the global scale, trends in streamflow extremes show substantial regional variability. For example, Do et al. (2017) reported decreasing annual maximum streamflows in parts of North America, Australia, and Europe, while increases were observed in eastern North America and some regions of South America and southern Africa. Similarly, Blöschl et al. (2019) showed that flood trends across Europe are strongly influenced by regional hydroclimatic drivers, particularly winter precipitation and soil moisture conditions. These studies highlight the importance of analyzing hydroclimatic influences on peak flows within regional climatic contexts, where different combinations of precipitation regimes, temperature patterns, and catchment storage processes may control runoff responses.

Chile provides an ideal natural laboratory for investigating such hydroclimatic variability. The country extends over approximately 38° of latitude and includes strong climatic gradients ranging from hyper-arid desert conditions in the Atacama Desert to humid temperate and cold climates in southern Patagonia. Annual precipitation varies from less than 1 mm in northern Chile to more than 3000 mm in southern regions, while elevation gradients associated with the Andes strongly influence hydrological processes. This diversity of climatic regimes produces a wide range of hydrological responses across Chilean catchments.

Recent studies have documented significant hydroclimatic changes in Chile. Boisier et al. (2018) reported multi-decadal declines in precipitation and streamflow across central-southern Chile, while Álvarez-Garretón et al. (2021) showed that the recent megadrought (2010–2020) amplified hydrological deficits through catchment storage and hydrological memory effects. Other studies have highlighted increasing temperatures, shifts in soil moisture regimes, and spatially heterogeneous changes in streamflow across the country (Oertel et al., 2020; Sangüesa et al., 2023). These findings suggest that hydroclimatic conditions influencing runoff generation may vary substantially across Chile’s diverse climate zones.

Despite these advances, important questions remain regarding how hydroclimatic variability relates to peak streamflow behavior across different climatic regimes. In particular, there is limited comparative analysis examining how hydroclimatic conditions associated with annual maximum streamflow events vary across Chile's contrasting climate zones. Understanding these associations is important for interpreting regional patterns of hydrological extremes and for improving the assessment of hydroclimatic influences on peak flows.

In this context, the present study analyses annual maximum streamflow records from 38 catchments distributed across a range of Köppen–Geiger climate regimes in Chile over the period 2000–2021. By combining hydrological observations with gridded precipitation, air temperature, and soil moisture datasets, the study examines the hydroclimatic conditions associated with peak streamflow across contrasting climatic settings.

Specifically, the objectives of this study are to:
(1) quantify temporal trends in annual maximum streamflow across Chilean catchments representing contrasting climate regimes;
(2) examine statistical associations between annual maximum streamflow and key hydroclimatic variables, including precipitation, air temperature, and soil moisture;
(3) assess how these hydroclimatic associations vary across different Köppen–Geiger climate zones.

By analyzing hydroclimatic conditions associated with peak streamflow across diverse climatic environments, this study contributes to improving the understanding of regional hydroclimatic variability and its association with extreme streamflow behavior. In addition, the comparative framework adopted here provides insights that are relevant for interpreting hydroclimatic controls on peak flows in other climatically heterogeneous regions."

- **MC2**. **Methodology is not appropriate to address Specific Objective 2**. Specific Objective 2 aims to "*identify dominant hydro-climatic controls on streamflow evolution by analysing relationships among streamflow, precipitation, temperature, and soil moisture variables*". While the identification of dominant hydro-climatic controls on streamflow evolution is indeed a relevant and interesting research question, particularly at the event scale, the methodological approach adopted in the manuscript is not adequate to support such inference. The study evaluates trends in annual maximum streamflow, precipitation, air temperature, and soil moisture, and subsequently computes the Spearman rank correlation coefficient among these variables. However, correlation does not imply causation, and the literature provides numerous examples of spurious correlations. High values of the Spearman coefficient alone do not constitute evidence of "*dominant* *hydro-climatic controls*" on streamflow evolution. To robustly identify dominant controls, a more rigorous experimental or modelling framework would be required, explicitly designed to disentangle causal relationships and quantify relative contributions. Such an approach is not implemented in the present manuscript.

R. We thank the reviewer for this important comment. We agree that correlation analysis alone does not allow the identification of causal relationships or "dominant hydro-climatic controls" on streamflow evolution. Our intention was not to infer causality but rather to explore statistical associations between hydroclimatic variables and annual maximum streamflow across different climate regimes.

To address this concern, the wording of Specific Objective 2 has been revised to avoid causal interpretation. The objective now explicitly focuses on analyzing statistical associations rather than identifying dominant controls. The revised objective reads:

"2- Examine statistical associations between annual maximum streamflow and key hydroclimatic variables, including precipitation, air temperature, and soil moisture."

Spearman's rank correlation was selected because it is a non-parametric method well suited to hydroclimatic datasets with relatively short records and non-normally distributed variables, which is commonly the case for extreme-value indices such as annual maxima. In addition, Spearman correlation evaluates monotonic relationships and is less sensitive to outliers than parametric correlation measures, making it appropriate for exploratory analyses of hydroclimatic variability.

Accordingly, the revised manuscript clarifies that the correlation analysis is used to examine statistical associations between peak streamflow and hydroclimatic conditions, rather than to identify causal drivers. Interpretations throughout the Results and Discussion sections have been revised to reflect this distinction.

- **MC3**. **Methodology is not appropriate to fully address Specific Objective 3**. Specific Objective 3 seeks to "*assess regional variations in climate–streamflow relationships to determine how different climate zones respond to hydro-climatic drivers*". However, as discussed in MC2, the methodology is limited to analysing trends in annual maximum streamflow, precipitation, air temperature, and soil moisture, followed by the computation of Spearman rank correlation coefficients among these variables. This approach allows the identification of regional differences in trends and in correlation coefficients among annual maximum variables. Nevertheless, it does not provide a robust framework for assessing variations in "*climate-streamflow relationships*". The manuscript does not clearly define how this relationship is conceptualized or

> evaluated, particularly with respect to the temporal scale adopted for the analysis. Moreover, the study does not explicitly define the "*hydro-climatic drivers*" assumed to control streamflow responses at the catchment scale. The analysis implicitly assumes that Köppen–Geiger climate classes, annual maximum precipitation, and air temperature are the primary climatic controls on annual maximum streamflow. However, it does not account for the potential modulating effects of catchment characteristics (e.g., soil properties, land cover, geology) or large-scale climatic teleconnections (e.g., ENSO, PDO, SAM). A more rigorous experimental design is required to clearly define and quantify the climate-streamflow relationship, specify the relevant temporal scale, and isolate the influence of different hydro-climatic drivers. Such an approach is not implemented in the current manuscript.

R. We thank the reviewer for this comment. We acknowledge that the original formulation of Specific Objective 3 and the methodological description did not sufficiently clarify how climate–streamflow relationships are conceptualized within the scope of this study, particularly with respect to the temporal scale of the analysis.

To address this concern, the objective has been reformulated to reflect the analysis's scope better. The new objective 3 is "3- Assess how these hydroclimatic associations vary across different Köppen–Geiger climate zones."

The revised objective now focuses on assessing how hydroclimatic conditions associated with peak flows vary across different climate regimes, rather than on identifying causal climate–streamflow relationships.

In addition, the methodological description has been clarified to better link hydroclimatic conditions to peak-flow occurrence. In the revised manuscript, for each catchment and year, the date of the annual maximum streamflow will be identified, and the associated hydroclimatic conditions (precipitation, temperature, and soil moisture) will be evaluated at that time and over antecedent periods. This event-based annual framework provides a more physically consistent basis for examining hydroclimatic conditions associated with peak flows across contrasting climate regimes.

The revised manuscript also clarifies the selection of the hydroclimatic variables used in the analysis. Precipitation, temperature, and soil moisture were selected because they represent key climatic factors influencing runoff generation and antecedent catchment conditions, and together, they provide a multivariable perspective on hydroclimatic variability affecting peak flows.

Finally, the manuscript now explicitly acknowledges that other factors, such as catchment characteristics and large-scale climate variability, may also influence streamflow responses. These aspects are discussed as potential sources of variability beyond the scope of the present analysis.

In the section “2.3.1 Variable definition and derivation” the new explanation about the variables begins with this:

“The selection of hydroclimatic variables was guided by their physical relevance to runoff generation processes and antecedent catchment conditions. Annual maximum streamflow (Q) was used as the primary response variable, representing extreme hydrological events. Precipitation (PP) was considered the main atmospheric forcing driving runoff generation, while air temperature (T) was included to account for its influence on processes such as evapotranspiration and snowmelt. Soil moisture (SM) was incorporated as an indicator of antecedent wetness conditions, reflecting catchment storage and hydrological memory.

To ensure a physically consistent linkage between hydroclimatic conditions and streamflow extremes, an event-based framework was adopted. For each catchment and year, the date of the annual maximum streamflow was identified, and the corresponding hydroclimatic variables were evaluated at that time. In addition, antecedent conditions were characterized by using aggregated variables over preceding periods, including accumulated precipitation over 7 days (PP7) and smoothed soil moisture over 3- and 7-day windows (SM3 and SM7), which represent short-term catchment memory and storage conditions influencing peak generation.”

- **MC4**. **Definition and naming of climate zones**. The Köppen–Geiger climate classification adopted in this study is based on an outdated, locally developed dataset (Sarricolea et al., 2017), rather than the state-of-the-art global classification provided by Beck et al. (2023). The use of a non-standard and older classification limits the comparability of the results with recent international studies published in leading hydrological journals. In addition, the manuscript does not assign descriptive names to the climate classes listed in the first column of Table 1. This omission significantly hinders the readability of the Results and Discussion sections. For example, line 524 refers to “*Mediterranean, temperate, and winter-rainfall climates*”, while line 545 mentions “*winter-rainfall climates -particularly Mediterranean, temperate and semi-arid regions*”. In neither case is it clear which of the nine climate classes defined in Table 1 is being referenced. To improve clarity and accessibility, I strongly recommend providing a concise textual description for each climate class (e.g., “*cold semi-arid/tundra*” instead of “*Bsk(s)-ET(s)-Bsk(s)(i)*”). This would greatly facilitate interpretation and ensure consistency throughout the manuscript.

  Beck, Hylke E., Tim R. McVicar, Noemi Vergopolan, Alexis Berg, Nicholas J. Lutsko, Ambroise Dufour, Zhenzhong Zeng, Xin Jiang, Albert IJM Van Dijk, and Diego G. Miralles. High-resolution (1 km) Köppen-Geiger maps for 1901–2099 based on constrained CMIP6 projections. Scientific Data 10, 724 (2023).https://doi.org/10.1038/s41597-023-02549-6.

R. We thank the reviewer for this helpful suggestion. We agree that the original manuscript did not provide sufficiently clear descriptions of the climate classes used in the analysis, which made the interpretation of the Results and Discussion sections more difficult.

Following this suggestion, Table 1 has been revised to include concise textual descriptions of each climate class in addition to the Köppen–Geiger classification codes. This modification improves readability and ensures that the same terminology is used consistently throughout the manuscript when referring to climate regimes.

In addition, we evaluated the Köppen–Geiger classification proposed by Beck et al. (2023) within the analyzed catchments to assess whether the use of the Sarricolea et al. (2017) dataset could influence the interpretation of the results. Because the analysis is conducted at the catchment scale, this comparison focused on the dominant climate class represented within each basin under both classifications.

The comparison indicates that the dominant climatic regimes identified in the study basins remain broadly consistent between both datasets. Minor differences arise primarily from two factors:

(i) The absence of local climatic modifiers in the Beck classification (e.g., altitude or seasonal precipitation indicators included in Sarricolea et al., 2017).

(ii) The higher spatial resolution of the Beck dataset, which captures altitudinal heterogeneity within some Andean catchments.

Importantly, these differences do not alter the dominant climatic regimes characterizing the analyzed catchments and therefore do not affect the interpretation of the results presented in this study. For this reason, the Sarricolea et al. (2017) classification remains appropriate for describing the regional climatic context of Chile while maintaining consistency with previous regional hydroclimatic studies.

The revised version of Table 1 is shown below.

Table 1. Köppen–Geiger climate classes represented in the analyzed catchments, including classification codes and descriptive climate names used consistently throughout the manuscript.

Zone	Climate description	Catchment		Climate zone importance			Predominant climate zones Code (%)	Area (km^2)	Elevation (m a.s.l)		Hydrological regime
		Name	Abbr.	First	Second	Third			Min	Max	
ET (w)	Tundra climate with summer rainfall	Río Desaguadero en Cotacotani	RDC	ET (w)	-	-	ET (w) (99.13%)	376	4528	6190	Pluvial
		Río Lauca en estancia El Lago	RLEL	ET (w)	-	-		583	4377	6245	Pluvial
		Río Lauca en Japu	RLJ	ET (w)	-	-		3278	3981	6273	Pluvial
		Río Guallatire en Guallatire	RGG	ET (w)	-	-		50	4226	5967	Pluvial
ET (w) - BSk (w)	Tundra climate with summer rainfall – Cold semi-arid climate with summer rainfall	Río Toconce antes represa sendos	RTARS	ET (w)	BSk (w)	-	ET (w) (81.04%) BSk (w) (13.78%)	156	3350	5623	Pluvial
		Río San Pedro en Parshall N°2 (BT. CHILEX)	RSPP2	ET (w)	BSk (w)	-		1250	3335	6123	Pluvial
		Río Salado en sifón Ayquina	RSSA	ET (w)	BSk (w)	-		807	2948	5604	Pluvial
		Río Salado A. J. Curti	RSAJC	ET (w)	BSk (w)	-		527	3115	5604	Pluvial
		Río Loa antes represa Lequena	RLRL	ET (w)	BSk (w)	-		2053	3323	6144	Pluvial
BSk (w) - ET (w)	Cold semi-arid climate with summer rainfall – Tundra climate with summer rainfall	Río San Pedro en Cuchabrachi	RSPC	ET (w)	BSk (w)	BWk (w)	BSk (w) (49.45%) ET (w) (42.23%)	1416	2561	5838	Pluvial
BSk (s) - ET (s)	Cold semi-arid climate with winter rainfall – Tundra climate with winter rainfall	Río Tascadero en desembocadura	RTD	BSk (s)	ET (s)	-	BSk (s) (70.81%) ET (s) (28.71%)	241	1229	3842	Pluvial/Nival
		Río Mostazal en Cuestecita	RMCU	BSk (s)	ET (s)	-		394	1252	4330	Pluvial/Nival
		Río Mostazal en Carén	RMCA	BSk (s)	ET (s)	-		640	701	4295	Pluvial/Nival
		Río Grande en Las Ramadas	RGLR	BSk (s)	ET (s)	-		569	1396	4299	Pluvial/Nival
		Río Grande en Cuyano	RGC	BSk (s)	ET (s)	-		1287	904	4246	Pluvial/Nival

Zone	Climate description	Catchment		Climate zone importance			Predominant climate zones Code (%)	Area (km^2)	Elevation (m a.s.l)		Hydrological regime
		Name	Abbr.	First	Second	Third			Min	Max	
ET (s) - Csb (h) - Csc	Tundra climate with winter rainfall – High-altitude warm summer mediterranean climate with winter rainfall - Warm summer mediterranean climate with winter rainfall	Estero Yerba Loca antes junta San Francisco	EYLSF	ET (s)	Csc	Csb (h)	ET (s) (33.36%) Csb (h) (32.17%) Csc (20.93%)	110	1354	5439	Pluvial/Nival
		Río San Francisco antes junta Estero Yerba Loca	RSFEYL	ET (s)	Csc	Csb (h)		139	1517	4868	Pluvial/Nival
		Río Molina antes junta San Francisco	RMSF	Csb (h)	Csc	ET (s)		300	1214	5345	Pluvial/Nival
		Estero Arrayán en La Montosa	EALM	Csc	Csb (h)	ET (s)		217	1049	3834	Pluvial/Nival
Csb	Warm summer mediterranean climate with winter rainfall	Río Vergara en Tijeral	RVT	Csb	-	-	Csb (93.33%)	2537	62	1777	Pluvial
		Río Rahue en Quebrada Culén	RRQC	Csb	-	-		671	108	729	Pluvial
		Río Dumo en Santa Ana	RDSA	Csb	-	-		393	276	1083	Pluvial
		Estero Chufquén en Chufquén	ECHCH	Csb	-	-		854	115	1691	Pluvial
		Río Lumaco en Lumaco	RLL	Csb	-	-		853	57	1369	Pluvial
		Río Traiguén en Victoria	RTV	Csb	-	-		94	330	855	Pluvial
		Río Quino en longitudinal	RQL	Csb	-	-		277	290	1668	Pluvial
Cfb (i) - Cfb	Temperate rainy climate with coastal influence – Temperate rainy climate	Río Negro en Las Lomas	RNLL	Cfb (i)	-	-	Cfb (i) (76.73%) Cfb (12.9%)	253	57	312	Pluvial
		Río Maullín en Las Quemas	RMLQ	Cfb (i)	Cfb	-		2278	17	2068	Pluvial
		Río Toro en Tegualda	RTT	Cfb (i)	-	-		339	93	357	Pluvial

- **MC5**. **Data sources**. The selection and treatment of the data sources are not adequately justified.

  First, the "Data sources" section (L175) states that "*The study focuses on identifying trends and correlations in extreme hydrological events*". However, the analysis is limited to annual maxima of selected variables, without a formal definition of extreme events (e.g., criteria for event start and end, minimum inter-arrival time, threshold selection). Annual maxima alone do not constitute an event-based extreme analysis.

R. We thank the reviewer for this comment. We acknowledge that the original wording in the manuscript may have suggested an event-based analysis of extreme hydrological events, which is not the approach adopted in this study.

The analysis is based on annual maximum values of streamflow and hydroclimatic variables, which represent commonly used indices of extreme conditions but do not constitute a formal event-based framework (e.g., defined by thresholds, event duration, or inter-arrival time). To avoid this ambiguity, the revised manuscript has been corrected to consistently refer to annual maximum streamflow and hydroclimatic conditions, rather than "extreme events".

In addition, the methodology has been improved to evaluate hydroclimatic variables on the date of occurrence of annual maximum streamflow, providing a more physically consistent linkage between peak flows and their associated conditions.

The manuscript has been revised to clarify that the analysis focuses on temporal trends and statistical associations of annual maximum streamflow and corresponding hydroclimatic conditions, rather than on the identification and characterization of individual hydrological events.

Annual maxima are widely used in hydrological studies as indicators of extreme conditions, particularly when consistent event definitions are not available across multiple catchments.

In the section "2.3.1 Variable definition and derivation" the new explanation about the variables begins with this:

"The selection of hydroclimatic variables was guided by their physical relevance to runoff generation processes and antecedent catchment conditions. Annual maximum streamflow (Q) was used as the primary response variable, representing extreme hydrological events. Precipitation (PP) was considered the main atmospheric forcing driving runoff generation, while air temperature (T) was included to account for its influence on processes such as evapotranspiration and snowmelt.

Soil moisture (SM) was incorporated as an indicator of antecedent wetness conditions, reflecting catchment storage and hydrological memory.

To ensure a physically consistent linkage between hydroclimatic conditions and streamflow extremes, an event-based framework was adopted. For each catchment and year, the date of the annual maximum streamflow was identified, and the corresponding hydroclimatic variables were evaluated at that time. In addition, antecedent conditions were characterized by using aggregated variables over preceding periods, including accumulated precipitation over 7 days (PP7) and smoothed soil moisture over 3- and 7-day windows (SM3 and SM7), which represent short-term catchment memory and storage conditions influencing peak generation."

> **Second**, the rationale for selecting the 38 streamflow stations is not provided. Some catchments are subject to significant anthropogenic regulation (e.g., the Lautaro reservoir), which, as acknowledged by the authors (L324–325), masks natural streamflow variability. If natural variability is altered, it is unclear how the study can robustly identify "*dominant hydro-climatic controls on streamflow*" (SO2). The manuscript does not explain why stations with near-natural regimes and consistent high-frequency (e.g., hourly) records across Chile were not prioritized.

R. We thank the reviewer for these comments. We acknowledge that the original manuscript did not clearly describe the rationale for catchment selection, the treatment of mixed climate classifications, or the influence of anthropogenic interventions.

In the revised manuscript, a new paragraph is considered in the methodology section explicitly describing the criteria used for catchment selection and climate classification (section "2.1 Study area"). The selection was designed to ensure the representation of contrasting hydroclimatic conditions across Chile, rather than to provide an exhaustive analysis of all available gauging stations. Catchments were selected based on (i) sufficient streamflow data availability to derive annual maximum series (with a minimum data coverage of 50% of the study period), (ii) availability of corresponding hydroclimatic variables, and (iii) representation of different Köppen–Geiger climate regimes.

Regarding climate classification, each catchment is now assigned to a Köppen–Geiger class based on the dominant climate type within its area. For catchments with mixed climate conditions, secondary and tertiary classes are also reported, allowing the representation of transition zones while maintaining a clear dominant classification.

We also acknowledge that some stations originally included corresponded to artificial channels or were affected by strong anthropogenic regulation. Following the reviewer's comment, stations located in artificial channels have been removed from the analysis. Additionally, catchments strongly influenced by reservoirs have also been excluded, including those affected by the Lautaro reservoir in the Copiapó basin and the Puclaro reservoir in the Elqui basin. These changes improve the consistency of the dataset in terms of representing natural streamflow variability.

Finally, we clarify that the objective of this study is to explore statistical associations between hydroclimatic variables and annual maximum streamflow across contrasting climatic settings, rather than to isolate strictly natural runoff processes. This distinction has been clarified in the revised manuscript.

The new explanation of catchment selection is below and will be part of the "Materials and methods" section of the Manuscript, particularly in the "2.1 Study area" section.

Catchment selection and climate classification

"Catchments were selected to represent contrasting hydroclimatic conditions across Chile, including differences associated with latitude, elevation, coastal influence, and precipitation regimes (winter- and summer-dominated). The objective was not to provide an exhaustive list of all available gauging stations, but rather to define a consistent, climatically representative subset suitable for comparative analysis of annual maximum streamflow.

The selection prioritized catchments with sufficient streamflow data availability to derive annual maximum series within the 2000–2021 period. Specifically, stations were required to have data coverage for at least 50% of the study period, ensuring a minimum number of annual maxima for robust analysis. In addition, all selected catchments include corresponding hydroclimatic variables (precipitation, temperature and soil moisture).

Each catchment was assigned to a Köppen–Geiger class based on the dominant climate type within its area. For catchments with mixed climate conditions, secondary and tertiary climate classes were also identified, allowing the inclusion of transition zones while preserving a clear dominant climatic signal.

Stations located in artificial channels were excluded, as they do not represent natural river flow conditions. Additionally, catchments strongly affected by anthropogenic regulation were excluded to improve the consistency of the dataset in representing hydroclimatic variability."

- Moreover, although L241–242 mention data gaps due to natural and operational factors, there is no information on the maximum allowable gap length, whether hourly data were consistently available throughout 2000-2021, or how temporal consistency was ensured.

R. We thank the reviewer for this comment. We acknowledge that the original manuscript did not clearly explain how missing streamflow data were handled before the derivation of the annual maximum series.

In this study, the original streamflow records contained gaps due to natural and operational factors. To ensure temporal consistency, missing data were reconstructed prior to the analysis using the infilling procedure described in Equations 11 and 12. This approach generated continuous hourly streamflow series over the study period, even during periods with limited or no original observations.

As a result, annual maximum streamflow values were derived from these reconstructed hourly series rather than from incomplete raw records. This clarification has been incorporated into the revised manuscript.

The explanation for this is now found in section "2.3.1 Variable definition and derivation", just above equations 11 and 12. This explanation is presented below.

"Original streamflow records contained gaps due to natural and operational factors. To ensure temporal consistency, missing data were reconstructed using regression relationships between neighboring stations (Eqs. 11 and 12). This procedure generated continuous hourly streamflow series over the study period, including periods with limited or no original observations. Annual maximum streamflow values were then derived from these reconstructed series."

- The use of logarithmic relationships (Equations 11 and 12) to fill gaps in annual maximum streamflows is not supported by references or validation analyses demonstrating their reliability.

R. Regarding the use of logarithmic relationships (Equations 11 and 12), we acknowledge that the original manuscript did not provide sufficient justification. In the revised version, the methodological description has been expanded to clarify that regression-based approaches are commonly used in hydrology for streamflow record extension and regionalization (Hirsch, 1982; Vogel and Stedinger, 1985; Razavi and Coulibaly, 2013). Logarithmic formulations were adopted to represent non-linear scaling relationships between stations, which are frequently observed in hydrological data and provide a robust empirical framework for infilling.

In the section "2.3.1 Variable definition and derivation" that appears below equations 11 and 12, the following paragraph is incorporated:

“Missing streamflow data were reconstructed using regression relationships between neighboring stations (Eqs. 11 and 12). Such approaches are commonly used in hydrology to extend streamflow records and to regionalize, where empirical relationships between gauged sites are used to estimate missing observations (Hirsch, 1982; Vogel and Stedinger, 1985; Razavi and Coulibaly, 2013).

Logarithmic regression models were adopted to represent power-law relationships between streamflow series, which are widely observed in hydrological processes and often provide improved performance compared to linear formulations. This approach allows capturing non-linear scaling between stations while maintaining a simple and robust empirical framework.”

- **Third**, the choice of the GLDAS-Noah v2.1 soil moisture product is not justified. No comparison is made with other widely used gridded datasets (e.g., ERA5, ERA5-Land, GLEAM, SMAP, ESA-CCI SM), nor is a literature review provided to support the suitability of GLDAS-Noah for Chile or South America. In addition, the manuscript does not specify which soil layer(s) from GLDAS-Noah were used.

R. We thank the reviewer for this comment. We acknowledge that the original manuscript did not provide sufficient justification for the selection of the GLDAS-Noah v2.1 soil moisture product.

In the revised manuscript, we have expanded the dataset description and clarified its suitability for this study. GLDAS-Noah has been widely used in hydrological and climate studies due to its spatial consistency, long temporal coverage, and integration of ground observations, satellite data and land-surface modelling (Rodell et al., 2004). Its continuous global coverage and temporal resolution make it particularly suitable for large-scale comparative analyses such as the one conducted in this study.

We note that the objective of this work is not to intercompare different soil moisture datasets, but to analyze hydroclimatic associations using a consistent data source across all catchments.

We have expanded the manuscript to include references supporting the use of GLDAS-Noah soil moisture data in hydrological applications. Previous studies have demonstrated its applicability at the basin scale and its consistency with other widely used soil moisture products, supporting its suitability for large-scale hydroclimatic analyses.

In addition, the revised manuscript now explicitly states that soil moisture from the top layer (0–10 cm) was used, as it is directly linked to surface hydrological processes and antecedent wetness conditions.

In section “2.2 Data sources”, the new paragraph on the source of soil moisture is as follows:

“Finally, soil moisture data were obtained from the Global Land Data Assimilation System version 2.1 (GLDAS-2.1; NASA GES DISC, 2020) (Rodell et al., 2004). GLDAS combines ground observations, satellite retrievals and land-surface models to provide globally consistent estimates of land-surface variables and has been widely applied and evaluated in hydrological studies at different spatial scales (Qi et al., 2015; Nayak et a., 2021). Previous studies have also shown that GLDAS-Noah soil moisture is consistent with satellite-derived products, supporting its use in large-scale hydroclimatic analyses (Liu et al., 2019).

In this study, soil moisture from the top soil layer (0–10 cm) was used, as it is closely related to surface hydrological processes and antecedent moisture conditions influencing runoff generation. The dataset covers 2000 to the present, with a temporal resolution of 3 hours and a spatial resolution of 0.25°. For each catchment, soil moisture values were extracted from all grid cells overlapping the basin and aggregated to the catchment scale using an area-weighted average.”

For each catchment, soil moisture values were extracted from intersecting grid cells and aggregated to the catchment scale.”

- **Fourth**, the study period (approximately 20 years) is short for robust trend detection in annual maxima (the core of this manuscript). The potential limitations associated with such a short record length are not discussed. This is a critical issue for a study focused on trend analysis, and it requires either a detailed justification or the use of datasets with longer temporal coverage.

R. We acknowledge that the relatively short length of the study period represents a limitation for trend detection, particularly for annual maximum streamflow, which is inherently highly variable. As suggested, we have strengthened the manuscript to discuss this limitation more explicitly.

The selected period (2000–2021) corresponds to the maximum temporal overlap among all datasets used (streamflow, CR2MET precipitation and GLDAS soil moisture), ensuring methodological consistency across variables. Extending the analysis would require combining datasets with different characteristics, potentially affecting comparability.

We have also clarified in the Discussion section that the results should be interpreted as reflecting recent hydroclimatic tendencies rather than long-term trends. In particular, the study period captures a climatically relevant interval in Chile, including the recent megadrought, which provides meaningful context for interpreting changes in annual maximum streamflow.

In the section “2.2 Data sources”, the new paragraph, just below the title, is as follows:

“The study period (2000–2021) was defined based on the temporal overlap between streamflow observations, gridded precipitation data (CR2MET) and soil moisture data from GLDAS-Noah, ensuring consistency across all analyzed variables. While longer records are generally preferable for trend detection in extreme hydrological variables, the selected period reflects the maximum common temporal coverage of the datasets used.

It is recognized that the relatively short record length introduces uncertainty in trend detection, particularly for annual maxima, which are inherently variable. Therefore, the results should be interpreted as indicative of recent hydroclimatic tendencies rather than long-term trends.”

In section “4. Discussion” at the end, there is now an explanation about the limitation of the study period:
“A limitation of this study is the relatively short record length (2000–2021), which may affect the robustness of trend detection, particularly for annual maxima that are inherently characterized by high interannual variability. Short time series can reduce the statistical power of trend tests and increase the sensitivity of results to individual extreme events.

However, the objective of this study is not to infer long-term historical trends, but rather to characterize recent hydroclimatic tendencies under current climate conditions. In this context, the selected period captures a climatically relevant interval that includes significant recent variability in Chile, including the megadrought (2010–2020), providing meaningful insight into contemporary streamflow behavior.”

- **Finally**, L196–197 indicate that catchment-scale averages of gridded datasets were computed using area-weighted approaches, but the software and specific procedures used are not described, which limits the reproducibility and transparency of the analysis.

R. We thank the reviewer for highlighting this point. We have clarified the methodology to improve reproducibility. Specifically, catchment boundaries were intersected with the gridded datasets using GIS tools, and area weights were computed based on the proportion of each grid cell within each catchment. Both fully and partially intersecting grid cells were included in the aggregation. The procedure was implemented using GIS processing and subsequent calculations in spreadsheet software.

A new paragraph is included in section “2.2 Data sources”, just below the lines mentioned by the reviewer, which reads as follows:

“Catchment boundaries were intersected with the gridded datasets using GIS tools, and the proportion of each grid cell falling within each catchment was computed. Area weights were derived from these proportions, allowing both fully and partially intersecting grid cells to be included in the aggregation. The procedure was implemented using GIS-based processing and subsequent calculations in spreadsheet software.”

- **MC6**. **Variable selection and definition**. The selection of variables such as $PP7_{daily,i}$, $SM3_{daily,i}$, $SM7_{daily,i}$, etc., appears arbitrary and lacks clear physical or methodological justification. For example, it is not evident why the annual maximum of a 3-hour soil moisture estimate ($SMmax_{annual}$) should be expected to correlate meaningfully with the annual maximum streamflow. The manuscript does not provide a conceptual or process-based explanation supporting these choices. If the objectives are to “*identify dominant hydro-climatic controls on streamflow evolution*” (SO1) and to “*assess regional variations in climate-streamflow relationships*” (SO2), a more appropriate approach would be to analyse the specific precipitation events that trigger the annual maximum streamflow at each catchment. Such an event-based framework would allow a clearer linkage between forcing and response. Conversely, if annual maxima of precipitation, streamflow, and soil moisture are treated as independent variables, without explicitly accounting for causal relationships, then it would be preferable to employ widely recognised extreme precipitation indices (e.g., Rx1day, Rx5day, R95pTOT, PRCPTOT). Using established indices would enhance comparability with the international literature and facilitate positioning the findings within the broader context of extreme hydroclimatic research.

R. We thank the reviewer for this comment. We agree that the original formulation of the methodology did not sufficiently clarify the physical basis for selecting hydroclimatic variables or for their temporal representation. To address this, the methodology has been revised to adopt an event-based framework. Specifically, for each catchment and year, the date of the annual maximum streamflow (Qmax) is identified, and the corresponding hydroclimatic conditions (precipitation, temperature, and soil moisture) are evaluated at that time, along with antecedent periods.

Within this framework, the selected variables are physically interpreted as follows: precipitation represents the primary atmospheric forcing driving runoff generation; temperature accounts for thermodynamic controls such as evapotranspiration and snowmelt processes; and soil moisture reflects antecedent wetness conditions and catchment storage, representing hydrological memory. Aggregated variables such as 7-day accumulated precipitation (PP7) and smoothed soil moisture over 3- and 7-day windows (SM3 and SM7) are used to characterize short-term antecedent conditions influencing peak flow generation.

This revised approach provides a more physically consistent linkage between hydroclimatic forcing and streamflow response, addressing concerns about the interpretation of independent annual maxima. While we acknowledge the usefulness of standard extreme precipitation indices (e.g., Rx1day, Rx5day), the adopted event-based framework allows a more direct assessment of hydroclimatic conditions associated with observed peak flows in each catchment.

In the section "2.3.1 Variable definition and derivation," the new explanation about the variables begins with this:

"The selection of hydroclimatic variables was guided by their physical relevance to runoff generation processes and antecedent catchment conditions. Annual maximum streamflow (Q) was used as the primary response variable, representing extreme hydrological events. Precipitation (PP) was considered the main atmospheric forcing driving runoff generation, while air temperature (T) was included to account for its influence on processes such as evapotranspiration and snowmelt. Soil moisture (SM) was incorporated as an indicator of antecedent wetness conditions, reflecting catchment storage and hydrological memory.

To ensure a physically consistent linkage between hydroclimatic conditions and streamflow extremes, an event-based framework was adopted. For each catchment and year, the date of the annual maximum streamflow was identified, and the corresponding hydroclimatic variables were evaluated at that time. In addition, antecedent conditions were characterized by using aggregated variables over preceding periods, including accumulated precipitation over 7 days (PP7) and smoothed soil moisture over 3- and 7-day windows (SM3 and SM7), which represent short-term catchment memory and storage conditions influencing peak generation."

- **MC7**. **Unnecessary figures**. The maps presented in the Results section (Figures 2–8) do not display spatially continuous hydrological variables. Instead, they represent discrete catchment-based results. As such, the current map format is unnecessarily repetitive and could be consolidated into one or two multi-panel figures covering the entire study area (Chile). Each

> catchment could be represented by a single symbol, coloured (e.g., brown for decreasing trends, blue for increasing trends) and left blank when no statistically significant trend is detected. This would improve clarity, reduce redundancy, and facilitate comparison across variables. Even in their current form, some potentially interesting spatial patterns are visible; for example, a single catchment showing a decreasing trend among predominantly non-significant trends (Figure 2b), or clusters of catchments with decreasing trends surrounded by others without significant trends (Figure 2h). However, these spatial configurations are not analysed or discussed in the manuscript. A more focused and interpretative discussion of such patterns would substantially strengthen the Results section.

R. We thank the reviewer for this valuable comment regarding the presentation of the results. We agree that the original maps (Figures 2–8), based on individual catchment polygons, were unnecessarily repetitive and did not fully exploit the dataset's spatial perspective. In response, we have redesigned the figures to present the results at the national scale using a unified map of Chile, where each catchment is represented by a single symbol indicating the trend direction and statistical significance. This new representation substantially improves clarity, reduces redundancy, and facilitates comparison across variables, as the reviewer suggested. The revised figures have been incorporated into the manuscript as Figure 3 and Figure 4.

In section “3.1 Trend analysis”, the new figures are the following two:

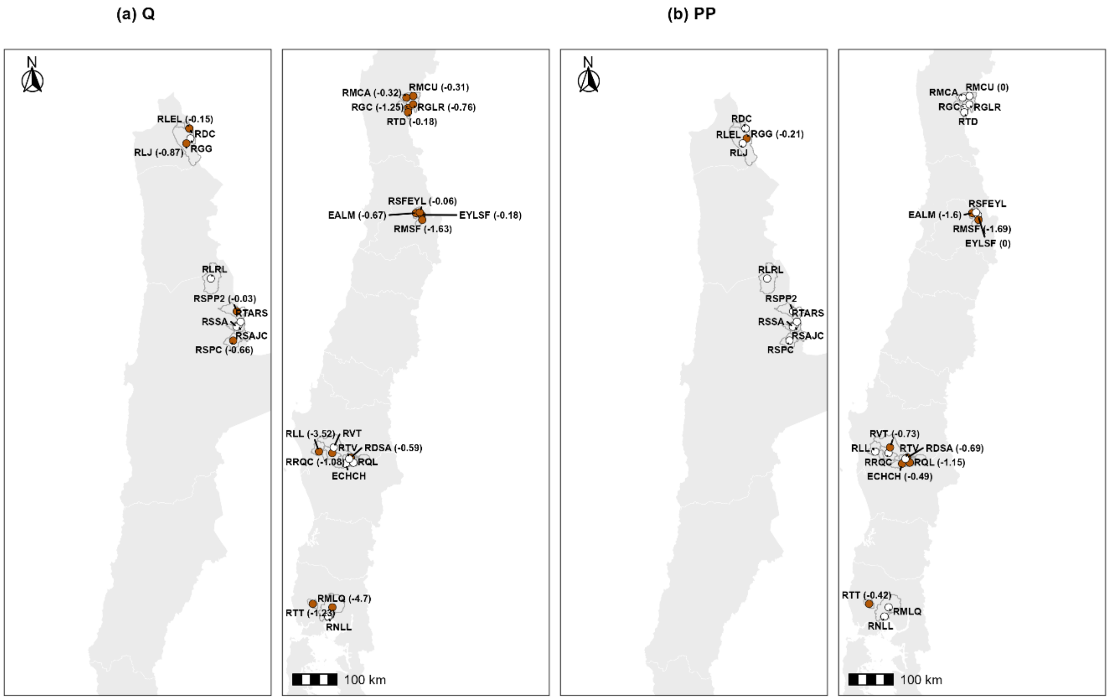

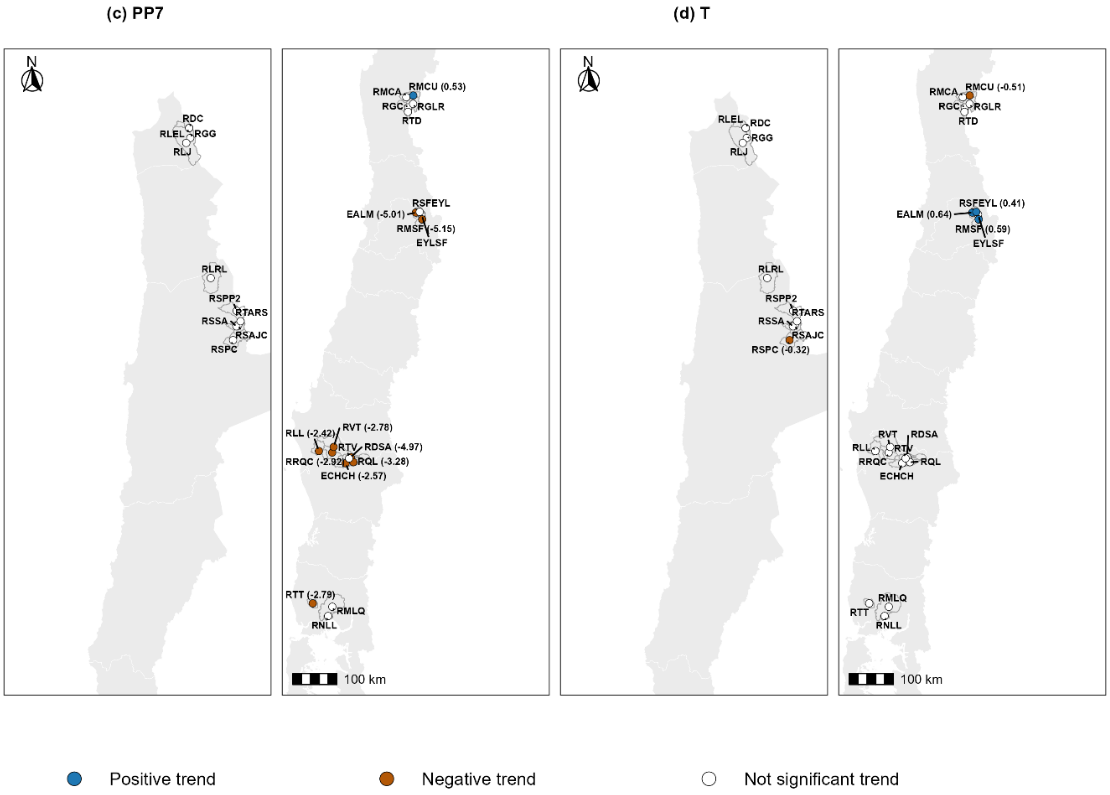

Figure 3. Trends in annual maximum streamflow and associated hydroclimatic variables (precipitation, 7-day accumulated precipitation and temperature) for the period 2000–2021. Values in parentheses next to the catchment labels indicate the Theil–Sen slope. The Theil–Sen slope is expressed in units per year: (a) Q in $m^3\ s^{-1}\ yr^{-1}$, (b) PP in $mm\ yr^{-1}$, (c) PP7 in $mm\ yr^{-1}$, and (d) T in $°C\ yr^{-1}$.

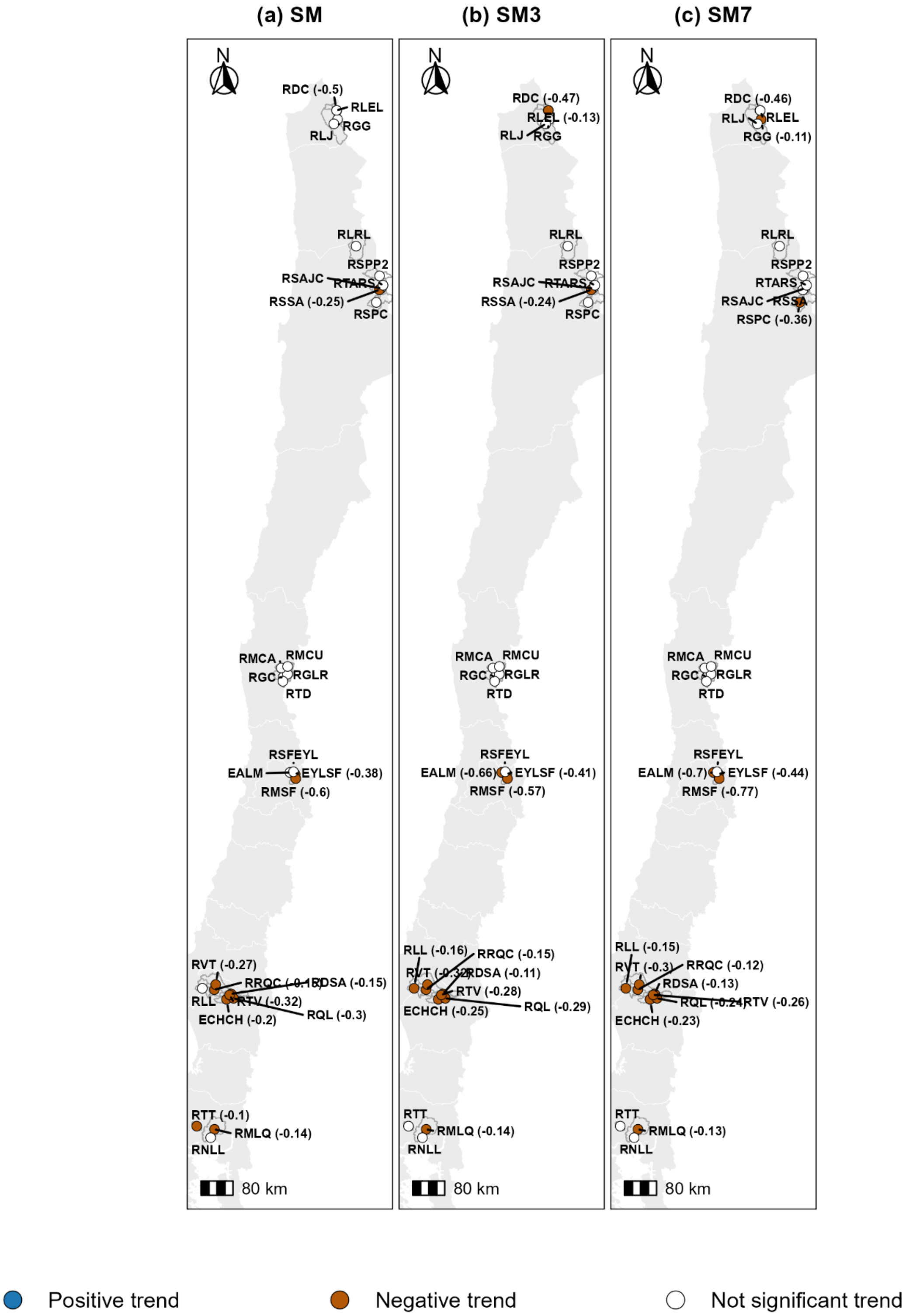

Figure 4. Trends in soil moisture and its smoothed variants (3-day and 7-day moving averages) for the period 2000–2021. Values in parentheses next to the catchment labels indicate the Theil–Sen slope. The Theil–Sen slope is expressed in units per year: (a) SM in mm yr^{-1}, (b) SM3 in mm yr^{-1}, and (c) SM7 in mm yr^{-1}

We thank the reviewer for highlighting the need for a more explicit interpretation of spatial patterns in the results. We agree that, although such patterns were visible in the original figures, they were not sufficiently analyzed or discussed.

In the revised manuscript, we have incorporated a focused interpretation of the spatial distribution of trends in the "3. Results" section. We now explicitly describe the presence of (i) isolated catchments with significant trends surrounded by non-significant neighbors and (ii) clusters of adjacent catchments exhibiting consistent negative trends. This additional analysis highlights the spatial heterogeneity of the observed responses and provides a clearer distinction between regional-scale hydroclimatic signals and locally modulated behavior. These additions strengthen the interpretation of the results by explicitly linking the mapped patterns to underlying hydroclimatic controls, as the reviewer suggested.

In section "3.1 Trend analysis", a new paragraph is added:

"In addition to the general patterns described above, the spatial distribution of trends reveals localized configurations that provide further insight into the behavior of extreme hydroclimatic variables. In several cases, individual catchments exhibiting significant decreasing trends are surrounded by neighboring basins with non-significant results, indicating spatial heterogeneity in the response of extremes. Conversely, clusters of adjacent catchments with consistent negative trends are observed, particularly in mediterranean (**Csb** and ET(s)–Csb(h)–Csc) and temperate (**Cfb(i)**–Cfb) regions, suggesting the presence of coherent regional-scale signals. These patterns indicate that, while large-scale hydroclimatic forcing governs the dominant trends, local factors such as catchment characteristics, elevation, or coastal influence may modulate their magnitude and statistical significance."

- **MC8**. **Results and Discussion sections are difficult to follow**. In addition to the issues raised in MC4 regarding the ambiguous use of climate zone terminology, two further aspects substantially limit the clarity of the Results and Discussion sections. **First**, the naming of variables is often ambiguous, preventing a clear understanding of what is being analysed. For example, L89 refers to "*Annual maximum soil moisture trends (Fig. 6)*" without specifying whether this corresponds to $SMmax_{annual}$, $SM3max_{annual}$, or $SM7max_{annual}$. Similar ambiguity appears in references to annual maximum precipitation (e.g., L339, Figure 3). Precise and consistent variable naming is essential for clarity, particularly when multiple related indices are introduced. Second, several interpretative statements are not clearly linked to supporting figures or tables. For instance, the statement "*In summer-rainfall climates, however, the signal is weaker or even positive*" (L435-436) does not specify which of the nine climate classes listed in Table 1 are being referenced, nor what the signal is being compared against. Likewise, "*The hydro-climatic patterns*

> *identified in the Mediterranean and temperate zones of Chile...*” (L454) lacks a clear correspondence with the climate classes defined earlier. Statements such as “*Overall, the results confirm the central role of precipitation...*” (L469) and “*Streamflow exhibits strong positive correlations with accumulated precipitation*” (L475-476) are not explicitly tied to a specific figure or table that demonstrates these findings. To improve readability and scientific rigour, all interpretative claims should explicitly reference the corresponding figures or tables, and terminology should be used consistently and unambiguously throughout the manuscript.

We thank the reviewer for this detailed and constructive comment. We agree that the clarity of the Results and Discussion sections can be improved by using more precise terminology and stronger linking between interpretations and supporting figures.

In the revised manuscript, we have addressed these issues in three main ways. First, variable naming has been standardized and clarified throughout the text. We now consistently distinguish between soil moisture variables (SM, SM3, and SM7) and precipitation variables (PP and PP7), and ambiguous expressions such as “annual maximum soil moisture” or “precipitation” have been replaced with the corresponding explicitly defined indices.

Second, references to climate zones have been made more explicit and consistent. Whenever broader terms such as “mediterranean”, “temperate”, or “summer-rainfall” climates are used, they are now clearly linked to the specific Köppen–Geiger classes defined in Table 1, ensuring that all interpretations can be unambiguously traced to the corresponding climate groups.

Third, we have revised the Results and Discussion sections to ensure that all interpretative statements are explicitly supported by references to the relevant figures or tables. This improves the traceability of the analysis and strengthens the scientific rigor of the manuscript.

These revisions substantially improve the readability and internal consistency of the manuscript, as well as the transparency of the interpretation of results.

In section “3. Results” there is a new introductory paragraph that clarifies the nomenclature of the variables:

“Hereafter, soil moisture variables are referred to as SM (3-hourly), SM3 (3-day moving average), and SM7 (7-day moving average), and precipitation variables as PP (daily maximum) and PP7 (7-day accumulated precipitation).”

The following section illustrates how variable naming, climate zone references, and figure references have been clarified in the revised manuscript.:

“In mediterranean climates (**Csb** and ET(s)–Csb(h)–Csc), annual maximum streamflow (Q) exhibits predominantly negative trends (Fig. 2 (a)), with several catchments showing statistically significant declines. In contrast, in summer-rainfall climates (**ET(w)**, **ET(w)**–BSk(w) and BSk(w)–ET(w)), trends are generally weaker and mostly non-significant (Fig. 2). Similarly, precipitation indices, including daily maxima (PP) and 7-day accumulated precipitation (PP7), display consistent decreasing trends across winter-rainfall climates (Fig. 2 (b,c)), reinforcing the spatial coherence of hydroclimatic changes.”

About the specific examples given by the revisor, the new versions are:

“In summer-rainfall climates (**ET(w)**, **ET(w)**–BSk (w) and BSk (w)–ET (w)), however, the signal is weaker or even positive”.

“The hydro-climatic patterns identified in the mediterranean (**Csb** and ET(s)–Csb(h)–Csc) and temperate (**Cfb(i)**-Cfb) zones of Chile...”

“Overall, the results confirm the central role of PP (Fig. 9-10)...”

“Streamflow exhibits strong positive correlations with PP7 (Fig. 9-10)”

Figures 9 and 10 will change the numeration in the final Manuscript.

- **MC9. Unsupported claims in the Results and Discussion sections**. The Results and Discussion sections contain several statements that are not supported by analyses presented in the manuscript. In multiple cases, interpretations extend beyond the scope of the data and methods described. Examples include:

- “*They are further modulated by elevation*” (L344). The role of elevation was not analysed or quantified in the study.
- “*Results suggest that in drier summer-rainfall regions, irregular rainfall events may counterbalance drying tendencies when soil moisture is measured at a three-hour resolution*” (L396-397). Rainfall events were neither formally defined nor analysed.
- “*In temperate rainy climates (Cfb(i)–Cfb), negative soil moisture trends were also present, albeit weaker than in arid winter-rainfall regions*” (L402-403). The relative magnitude (intensity) of trends was not evaluated in a way that supports this comparison.

- "*With the most substantial decreases occurring in the north, indicating progressive soil drying driven by reduced rainfall and snowmelt*" (L414-415). Snowmelt processes were not analysed, and no evidence was presented demonstrating that reduced rainfall or snowmelt drives the reported soil moisture trends.
- "*Soil moisture emerges as an intermediate variable, strongly associated with precipitation, and in Mediterranean and temperate climates, it modulates runoff responses*" (L471-472). The manuscript does not analyse how soil moisture modulates runoff responses to precipitation.
- "*The results here indicate that enhanced evapotranspiration instead reduces streamflow availability*" (L540-541). Evapotranspiration was not analysed.
- "*However, in purely tundra climates, soil moisture shows weak or even opposite signals because snow and frozen ground dominate the hydrological response…*" (L551-552). Snow and frozen ground processes were not evaluated.
- "*The spatial variability of soil moisture trends reflects the interplay between precipitation seasonality …*" (L554-555). Spatial variability of soil moisture trends was not explicitly analysed beyond catchment-level summaries.
- "*However, this is partially mitigated by consistency with longer records (Boisier et al., 2018)*" (L610–611). No quantitative comparison with longer records is presented to substantiate this claim.

- Overall, several interpretations introduce processes (elevation effects, event dynamics, snowmelt, evapotranspiration, frozen soils) that were not analysed within the methodological framework of the study. All interpretative statements should be directly supported by the presented analyses, or clearly framed as hypotheses or speculative interpretations requiring further investigation.

R. We thank the reviewer for this important comment. We agree that several interpretative statements in the original manuscript extended beyond the scope of the analyses presented.

In the revised manuscript, we have carefully reviewed the Results and Discussion sections and removed or reformulated statements that were not directly supported by the data and methods. In particular, references to processes such as elevation effects, event-scale dynamics, snowmelt, evapotranspiration, and frozen soil conditions have been either removed or rephrased to avoid unsupported causal interpretations.

Where appropriate, some statements have been retained but reframed more cautiously as potential explanations, clearly presented as hypotheses rather than conclusions. Overall, the revised manuscript now ensures that all interpretations remain strictly consistent with the statistical analyses conducted (trend analysis and correlation-based relationships), without introducing processes that were not explicitly evaluated.

These revisions substantially improve the scientific rigor of the manuscript and ensure that all conclusions are directly supported by the presented results.

The revised Results and Discussion sections are presented below to reflect the changes described above.

3 Results

This section presents the main findings of the study regarding the temporal evolution of streamflow regimes and their relationships with meteorological drivers and soil moisture across 29 catchments in Chile. Finally, the correlation analysis integrates these variables to assess the strength and direction of their associations across contrasting climatic zones. The outcomes are reported at both the catchment and climatic-zone scales, highlighting both consistent patterns and regional differences. Together, these results provide a basis for identifying the dominant hydroclimatic controls on streamflow variability across diverse climatic conditions. Hereafter, soil moisture variables are referred to as SM (3-hourly), SM3 (3-day moving average) and SM7 (7-day moving average) and precipitation variables as PP (daily maximum) and PP7 (7-day accumulated precipitation).

3.1 Trend analysis

Results for maximum streamflow, precipitation, 7-day accumulated precipitation, and temperature are presented in Figure 3, whereas results for soil moisture, 3-day averaged soil moisture, and 7-day averaged soil moisture are shown in Figure 4.

Figure 3. Trends in annual maximum streamflow and associated hydroclimatic variables (precipitation, 7-day accumulated precipitation and temperature) for the period 2000–2021. Values in parentheses next to the catchment labels indicate the Theil–Sen slope. The Theil–Sen slope is expressed in units per year: (a) Q in $m^3 s^{-1} yr^{-1}$, (b) PP in mm yr^{-1}, (c) PP7 in mm yr^{-1}, and (d) T in °C yr^{-1}.

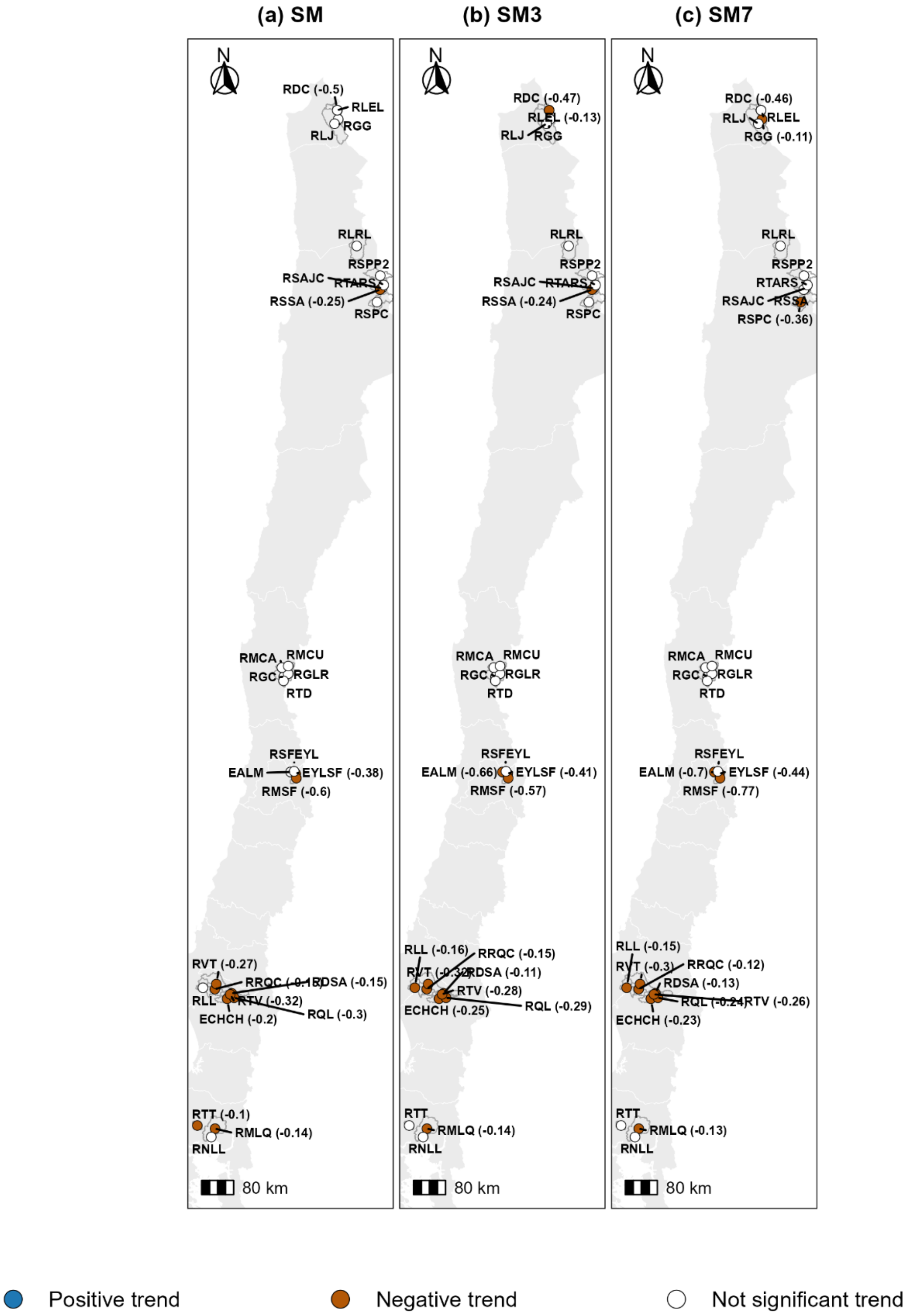

Figure 4. Trends in soil moisture and its smoothed variants (3-day and 7-day moving averages) for the period 2000–2021. Values in parentheses next to the catchment labels indicate the Theil–Sen slope. The Theil–Sen slope is expressed in units per year: (a) SM in mm yr^{-1}, (b) SM3 in mm yr^{-1}, and (c) SM7 in mm yr^{-1}.

The analysis of annual maximum streamflow for the period from 2000 to 2021 shows predominantly negative trends across the study catchments (Fig. 3a), particularly in the mediterranean (Csb and ET(s)–Csb(h)–Csc) and temperate (Cfb(i)–Cfb) climatic zones, where significant and large-magnitude declines prevail (Fig. 3a). Within the Csb zone, decreases are concentrated in the central and western sectors of the study area, which are almost entirely dominated by warm summer mediterranean climates with winter rainfall. In the ET(s)–Csb(h)–Csc zone, the steepest declines occur in catchments influenced by high-altitude warm-summer and cold-summer mediterranean climates, with a secondary contribution from tundra areas. The shared presence of mediterranean regimes suggests that these regions are susceptible to reductions in precipitation, with higher elevation modulating the magnitude of these declines.

In temperate rainy zones (Cfb(i)–Cfb), significant negative trends are also evident, especially in the largest catchments. For example, the RMLQ catchment exhibits one of the steepest declines, underscoring the marked reduction in streamflow extremes in temperate coastal-influenced climates, though this effect extends partially inland. Overall, regions characterised by intense winter rainfall display the most consistent downward signals in streamflow maxima.

In semi-arid transition zone (BSk(s)–ET(s)), negative slopes are also observed but tend to be more heterogeneous and less frequently significant. In the BSk(s)–ET(s) zone, more substantial declines occur in the Río Grande catchments, where the cold semi-arid climate with winter rainfall predominates. At the same time, weaker signals are detected further south, where the influence of the tundra slightly increases.

In one of the northern study areas (BSk(w)–ET(w)), only slight downward trends were found, likely linked to localised summer rainfall events. Similarly, in the ET(w)–BSk(w) zone, trends were dispersed and mostly non-significant, with both weak negative and occasional positive slopes, suggesting the influence of localised extreme summer events rather than consistent climate-driven signals.

In tundra-dominated zones (ET(w)), significant declines appear mainly in larger catchments, where decreases intensify with catchment size. These summer-rainfall regions are primarily influenced by tundra climates, with minimal contributions from semi-arid zones.

In summary, the most robust signal is the consistent decline in maximum streamflow in mediterranean and temperate climates, followed by other winter-rainfall climates and, to a lesser extent, tundra climates. These patterns align with broader hydro-climatic drivers, namely reduced precipitation and increasing temperatures across central and southern Chile (Oertel et al. 2020; Salazar et al. 2024).

Annual maximum precipitation shows a predominantly negative signal across the study area, with the strongest and most consistent decreases in the mediterranean (Csb and ET(s)–Csb(h)–Csc) and temperate (Cfb(i)–Cfb) zones (Fig. 3b). In the Csb zone, significant declines are in the catchments that does not show significant streamflow trends. In the ET(s)–Csb(h)–Csc zone, all catchments exhibited significant and large-magnitude declines, making this the most affected climatic setting. These patterns are consistent with the influence of winter-rainfall mediterranean climates.

In semi-arid winter-rainfall zone (BSk(s)–ET(s)), significant negative trends were not detected, despite the winter-rainfall regime, because of the semi-arid influence. In tundra and summer-rainfall influenced zones (ET(w)–BSk(w) and BSk(w)–ET(w)), precipitation trends were weaker, more heterogeneous, and mostly non-significant, highlighting the of summer convective rainfall in these regions. In the temperate rainy zone (Cfb(i)–Cfb), significant negative slopes were found, particularly in coastal-influenced catchments such as Río Toro, reinforcing the evidence of sustained precipitation declines in oceanic climates.

Seven-day accumulated precipitation provided an even stronger and more consistent signal of decline (Fig. 3c). In the Csb zone, a larger number of catchments displayed significant decreases. In the ET(s)–Csb(h)–Csc zone, the catchments showed reinforced negative slopes, confirming this as the climatic zone with the most pronounced reduction in multi-day rainfall events. In temperate rainy zone (Cfb(i)–Cfb), the catchment closest to the coast also shifted from non-significant to significant, indicating that prolonged rainfall extremes are declining even in ocean-moderated regions. In semi-arid with winter rainfall zone (BSk(s)–ET(s)), the trend of seven-day precipitation was generally non-significant but the RMCU show an increasing trend. By contrast, in tundra and summer-rainfall regions (ET(w)–BSk(w), BSk(w)–ET(w) and ET(w)), signals remained weak and mostly non-significant, reaffirming the limited role of rainfall extremes in summer-rainfall dominated zones. These findings indicate that precipitation reductions affect not only isolated daily extremes but also longer-duration events, which are critical for runoff generation.

Temperature extremes exhibit a different signal, with modest and warming trend in some catchments and non-significant trend in almost all catchments (Fig. 3d). In ET(s)–-Csb(h)–Csc zone, upward trends were statistically significant in several catchments, reflecting regional warming in this transition zone. In semi-arid and tundra zones (BSk(s)–ET(s), ET(w)–BSk(w), BSk(w)–ET(w) and ET(w)), warming trends were generally non-significant and negative in some specific cases. In the BSk(w)–ET(w) temperature shows a decreasing trend, where semi-arid climate predominates more than tundra climate.

Overall, the results reveal a consistent hydro-climatic signal: precipitation extremes – both daily and accumulated – are declining in mediterranean and temperate (CSb, ET(s)–Csb(h)–Csc and Cfb(i)–Cfb), while temperature maxima are increasing across the entire study area.

Annual maximum soil moisture trends (Fig. 4a) are generally downward, although they are not as pronounced as those observed for streamflow and precipitation. Nonetheless, the drying signal is more evident than the warming detected in temperature extremes. In cold semi-arid climates with winter rainfall (BSk(s)–ET(s)), any catchment shows significant results soil moisture trends. In arid zone influenced by summer rainfall (ET(w)–BSk(w), BSk(w)–ET(w) and ET (w)), significant positive trends emerged in some specific catchments. In the ET(w)–BSk(w) zone, decreases were observed in the southern sector, which is dominated by tundra influence.

These results may reflect the high variability of rainfall in summer-rainfall regions, where intermittent precipitation inputs could influence soil moisture conditions despite overall drying tendencies, considering that tundra climates with summer rainfall did not display consistent significant changes, but rather a regional effect.

In the Csb zone, catchments exhibited downward slopes, while in the ET(s)–Csb(h)–Csc, results were even more significant in the EYLSF and RMSF catchments, indicating that the most pronounced soil moisture decreasing trends are in the mediterranean climates with winter rainfall. In temperate rainy climates (Cfb(i)–Cfb), negative soil moisture trends were also present, albeit weaker than in mediterranean winter-rainfall regions. These decreases are consistent with precipitation declines, highlighting a drying tendency even in traditionally humid environments.

Three-day averaged soil moisture (Fig. 4b) revealed that in the ET(w)–BSk(w) and ET(w) zones, specific downward trends remained. In the Cfb(i)–Cfb, significant decreases persisted, but smoothing attenuated their magnitude. In the Csb zone, all catchments exhibited negative slopes, albeit weaker than those in the three-hourly datasets, suggesting an overall reduction in soil moisture. In the ET(s)–Csb(h)–Csc, persist the soil moisture trends.

The seven-day-averaged soil moisture (Fig. 4c) confirmed the results from the three-day average, reinforcing the general patterns across the climate zones. The smoothing effect enabled more precise identification of regional tendencies, confirming drying in mediterranean and temperate climates (CSb, ET(s)–Csb(h)–Csc and Cfb(i)–Cfb). In contrast, summer-rainfall-dominated zones (ET(w)–BSk(w), BSk(w)–ET(w) and ET(w)) showed more heterogeneous trends.

Overall, soil moisture extremes are declining across most winter-rainfall climates (CSb, ET(s)–Csb(h)–Csc and Cfb(i)–Cfb), particularly in mediterranean and temperate regions, where precipitation reductions are acting. In summer-rainfall climates (ET(w)–BSk(w), BSk(w)–ET(w) and ET(w)), however, the signal is weaker, reflecting the irregular nature of precipitation events during that season.

In addition to the general patterns described above, the spatial distribution of trends reveals localized configurations that provide further insight into the behaviour of extreme hydroclimatic variables. In several cases, individual catchments exhibiting significant decreasing trends are surrounded by neighbouring basins with non-significant results, indicating spatial heterogeneity in the response of extremes. Conversely, clusters of adjacent catchments with consistent negative trends are observed, particularly in mediterranean (Csb and ET(s)–Csb(h)–Csc) and temperate (Cfb(i)–Cfb) regions, suggesting the presence of coherent regional-scale signals. These patterns indicate that, while large-scale hydroclimatic forcing governs the dominant trends, local factors such as catchment characteristics, elevation, or coastal influence may modulate their magnitude and statistical significance.

To provide an integrated view of the hydroclimatic tendencies identified across the study area, Table 2 summarises the direction and significance of trends for all variables and climatic zones.

Southern catchments, which are dominated by mediterranean and temperate winter-rainfall regimes (CSb, ET(s)–Csb(h)–Csc and Cfb(i)–Cfb), exhibit a higher proportion of significant negative trends in maximum precipitation (both daily and seven-day accumulations), streamflow, and soil moisture. By contrast, northern catchments, characterised by semi-arid and tundra summer-rainfall climates (ET(w)–BSk(w), BSk(w)–ET(w) and ET(w)), show more heterogeneous soil-moisture trends and fewer significant changes in precipitation and streamflow. This contrast highlights the dominant role of precipitation variability in shaping hydrological responses in winter-rainfall regions, whereas in northern zones, irregular summer rainfall buffer or counterbalance drying signals. In the south, synchronous declines in precipitation, streamflow, and soil moisture reflect a broader drying tendency driven by climatic forcing. Overall, the results indicate a pronounced drying tendency in central and southern Chile, where winter-rainfall climates prevail, highlighting the combined effects of reduced precipitation inputs and increasing temperatures on streamflow generation.

Table 2. Summary of trend directions and significance across climatic zones. Positive trends are shown in blue, negative trends in red, and non-significant trends are in black.

Zone	Number of stations	Q trend	PP trend	PP7 trend	T trend	SM trend	SM3 trend	SM7 trend
ET (w)	4	2/2	1/3	4	4	1/3	1/3	2/2
ET (w) - BSk (w)	5	1/5	5	5	5	1/4	1/4	5
BSk (w) - ET (w)	1	1	1	1	1	1	1	1
BSk (s) - ET (s)	5	5/0	1/4	1/4	1/4	5	5	5
ET (s) - Csb (h) - Csc	4	4/0	3/1	2/2	3/1	2/2	3/1	3/1
Csb	7	3/4	4/3	6/1	7	6/1	7/0	7/0
Cfb (i) - Cfb	3	2/1	1/2	1/2	3	2/1	1/2	1/2

The hydro-climatic patterns identified in the mediterranean and temperate zones of Chile mirror those observed in other winter-rainfall regions worldwide. In Southern Europe, widespread streamflow declines linked to warmer and drier conditions have been reported in Spain (Yeste et al., 2018), central Italy (Gentilucci and Hamed, 2023), and Cyprus (Myronidis et al., 2018), confirming the high sensitivity of mediterranean hydroclimates to concurrent decreases in precipitation and rising temperatures. Similar signals have been found in streamflow trends in semi-arid regions, where enhanced evapotranspiration offsets rainfall gains, as documented in northeastern Iran (Minaei and Irannezhad, 2018) and in arid and warm-dry areas of North America and Australia (Do et al., 2017). In contrast, high-elevation and snow-dominated systems show weak or mixed trends, consistent with observations from the Hindu Kush–Karakoram–Himalaya (Hasson et al., 2017) and northern China (Xu et al., 2024; Lu et al., 2025), where temperature exerts stronger control on runoff generation than precipitation. Overall, these international comparisons reinforce that the drying tendencies identified in central and southern Chile (Oertel et al., 2020; Sangüesa, 2023; Alvarez-Garretón et al., 2021) are part of a broader global pattern affecting winter-rainfall climates, as also emphasised by the IPCC (2023).

3.2 Correlation analysis

The correlation analysis provides insight into the relationships among streamflow and hydroclimatic conditions evaluated at the date of annual maximum streamflow. Overall, the results highlight the dominant role of precipitation, particularly seven-day accumulated precipitation (PP7), in shaping peak flow conditions across most catchments.

The correlation analysis provides insight into the significant relationships among streamflow and hydroclimatic conditions evaluated at the date of annual maximum streamflow. Overall, the results highlight the dominant role of precipitation, particularly seven-day accumulated precipitation (PP7), in shaping peak flow conditions across most catchments.

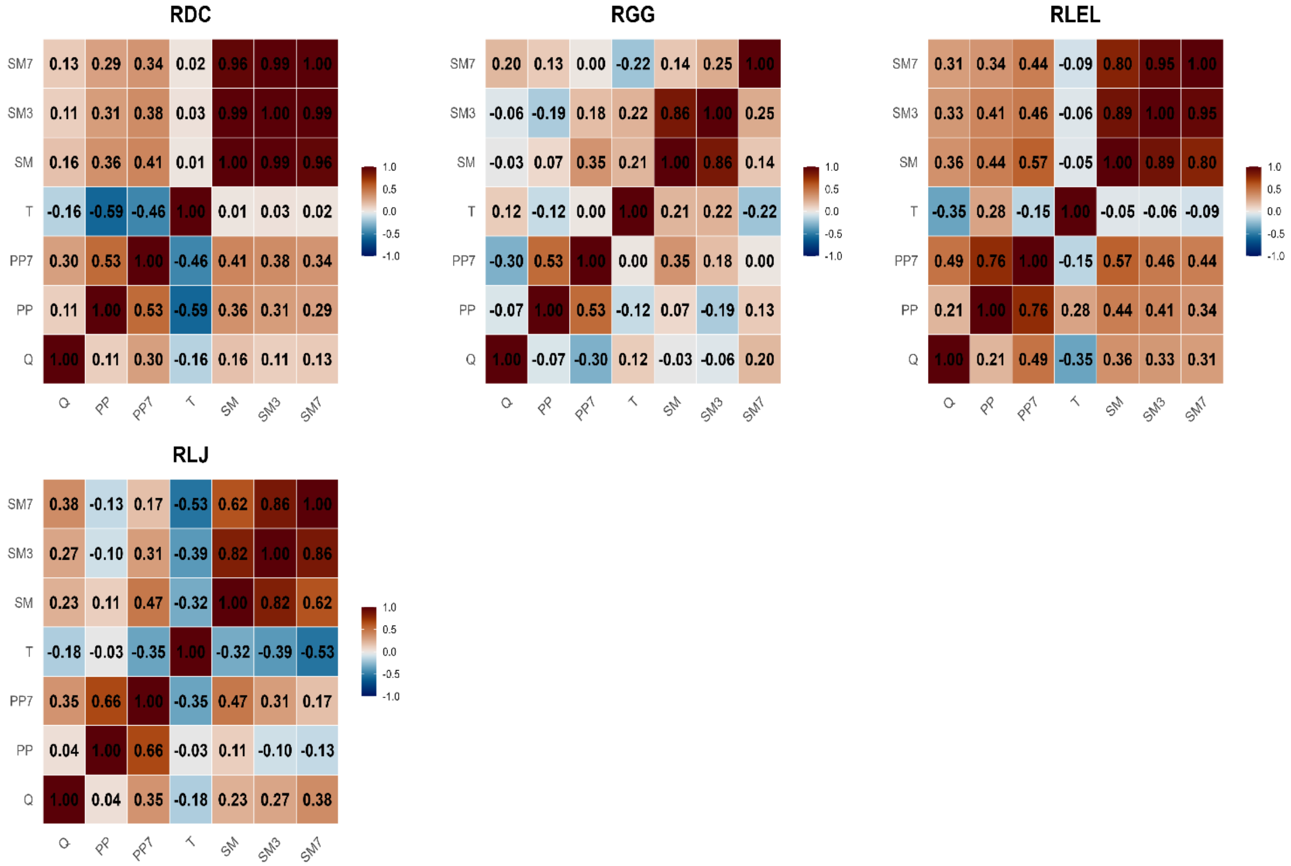

Figure 5. "ET(w)" correlation matrices for all combinations of variables.

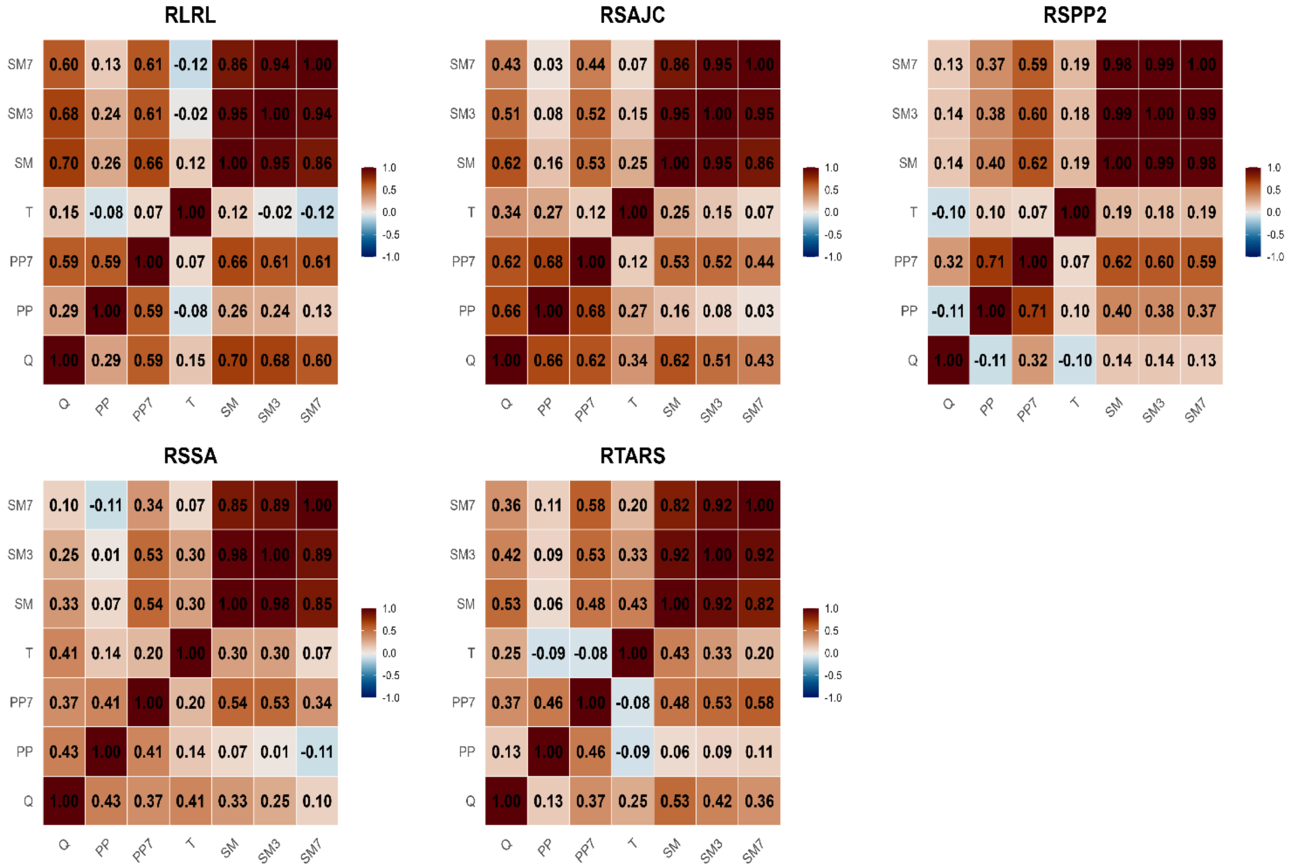

RLRL

	Q	PP	PP7	T	SM	SM3	SM7
SM7	0.60	0.13	0.61	-0.12	0.86	0.94	1.00
SM3	0.68	0.24	0.61	-0.02	0.95	1.00	0.94
SM	0.70	0.26	0.66	0.12	1.00	0.95	0.86
T	0.15	-0.08	0.07	1.00	0.12	-0.02	-0.12
PP7	0.59	0.59	1.00	0.07	0.66	0.61	0.61
PP	0.29	1.00	0.59	-0.08	0.26	0.24	0.13
Q	1.00	0.29	0.59	0.15	0.70	0.68	0.60

RSAJC

	Q	PP	PP7	T	SM	SM3	SM7
SM7	0.43	0.03	0.44	0.07	0.86	0.95	1.00
SM3	0.51	0.08	0.52	0.15	0.95	1.00	0.95
SM	0.62	0.16	0.53	0.25	1.00	0.95	0.86
T	0.34	0.27	0.12	1.00	0.25	0.15	0.07
PP7	0.62	0.68	1.00	0.12	0.53	0.52	0.44
PP	0.66	1.00	0.68	0.27	0.16	0.08	0.03
Q	1.00	0.66	0.62	0.34	0.62	0.51	0.43

RSPP2

	Q	PP	PP7	T	SM	SM3	SM7
SM7	0.13	0.37	0.59	0.19	0.98	0.99	1.00
SM3	0.14	0.38	0.60	0.18	0.99	1.00	0.99
SM	0.14	0.40	0.62	0.19	1.00	0.99	0.98
T	-0.10	0.10	0.07	1.00	0.19	0.18	0.19
PP7	0.32	0.71	1.00	0.07	0.62	0.60	0.59
PP	-0.11	1.00	0.71	0.10	0.40	0.38	0.37
Q	1.00	-0.11	0.32	-0.10	0.14	0.14	0.13

RSSA

	Q	PP	PP7	T	SM	SM3	SM7
SM7	0.10	-0.11	0.34	0.07	0.85	0.89	1.00
SM3	0.25	0.01	0.53	0.30	0.98	1.00	0.89
SM	0.33	0.07	0.54	0.30	1.00	0.98	0.85
T	0.41	0.14	0.20	1.00	0.30	0.30	0.07
PP7	0.37	0.41	1.00	0.20	0.54	0.53	0.34
PP	0.43	1.00	0.41	0.14	0.07	0.01	-0.11
Q	1.00	0.43	0.37	0.41	0.33	0.25	0.10

RTARS

	Q	PP	PP7	T	SM	SM3	SM7
SM7	0.36	0.11	0.58	0.20	0.82	0.92	1.00
SM3	0.42	0.09	0.53	0.33	0.92	1.00	0.92
SM	0.53	0.06	0.48	0.43	1.00	0.92	0.82
T	0.25	-0.09	-0.08	1.00	0.43	0.33	0.20
PP7	0.37	0.46	1.00	-0.08	0.48	0.53	0.58
PP	0.13	1.00	0.46	-0.09	0.06	0.09	0.11
Q	1.00	0.13	0.37	0.25	0.53	0.42	0.36

Figure 6. "ET(w)‑BSk(w)" correlation matrices for all combinations of variables.

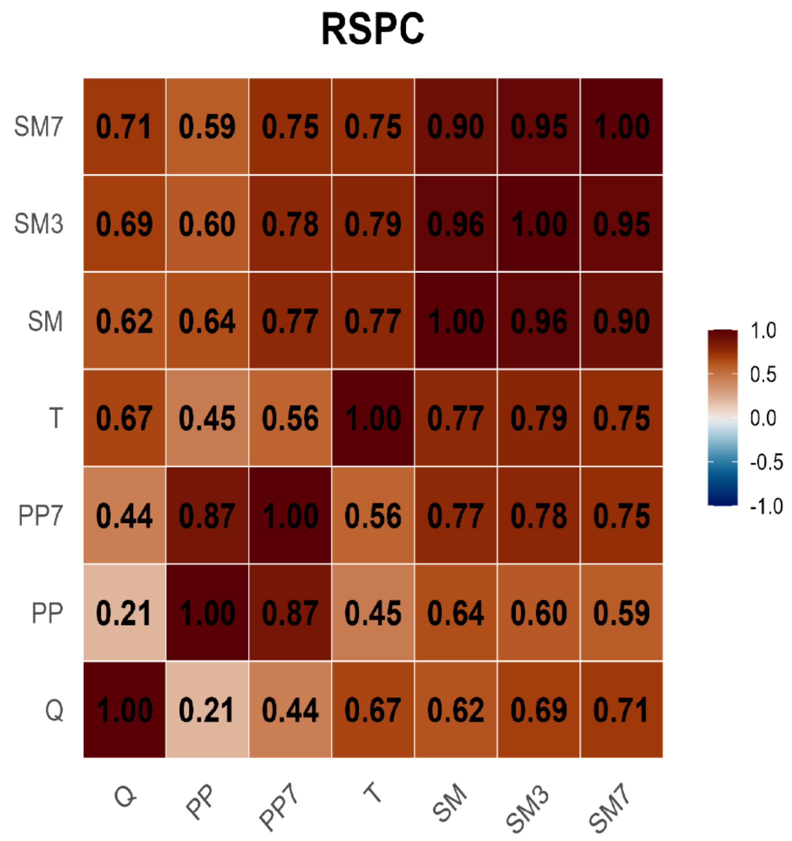

Figure 7. "BSk(w)‑ET(w)" correlation matrices for all combinations of variables.

In ET(w) and ET(w)–BSk(w) catchments (Fig. 5–6), streamflow is only weakly related to same-day precipitation, whereas its association with 7-day accumulated precipitation is generally more evident. Soil moisture also shows weak to moderate positive correlations with streamflow, particularly in the transition zone. By contrast, temperature exhibits mixed and mostly weak relationships, with no consistent sign across catchments. Overall, these patterns suggest that peak flows in these regimes are more closely associated with antecedent wetness and multi-day precipitation than with precipitation on the day of the event alone.

In the BSk(w)–ET(w) transition zone (Fig. 7), correlations are consistently high across all variables, including temperature. This strong coherence suggests that peak flow events occur under well-defined hydroclimatic conditions where precipitation, soil moisture and temperature co-vary. However, this behaviour may also reflect local characteristics and should be interpreted with caution.

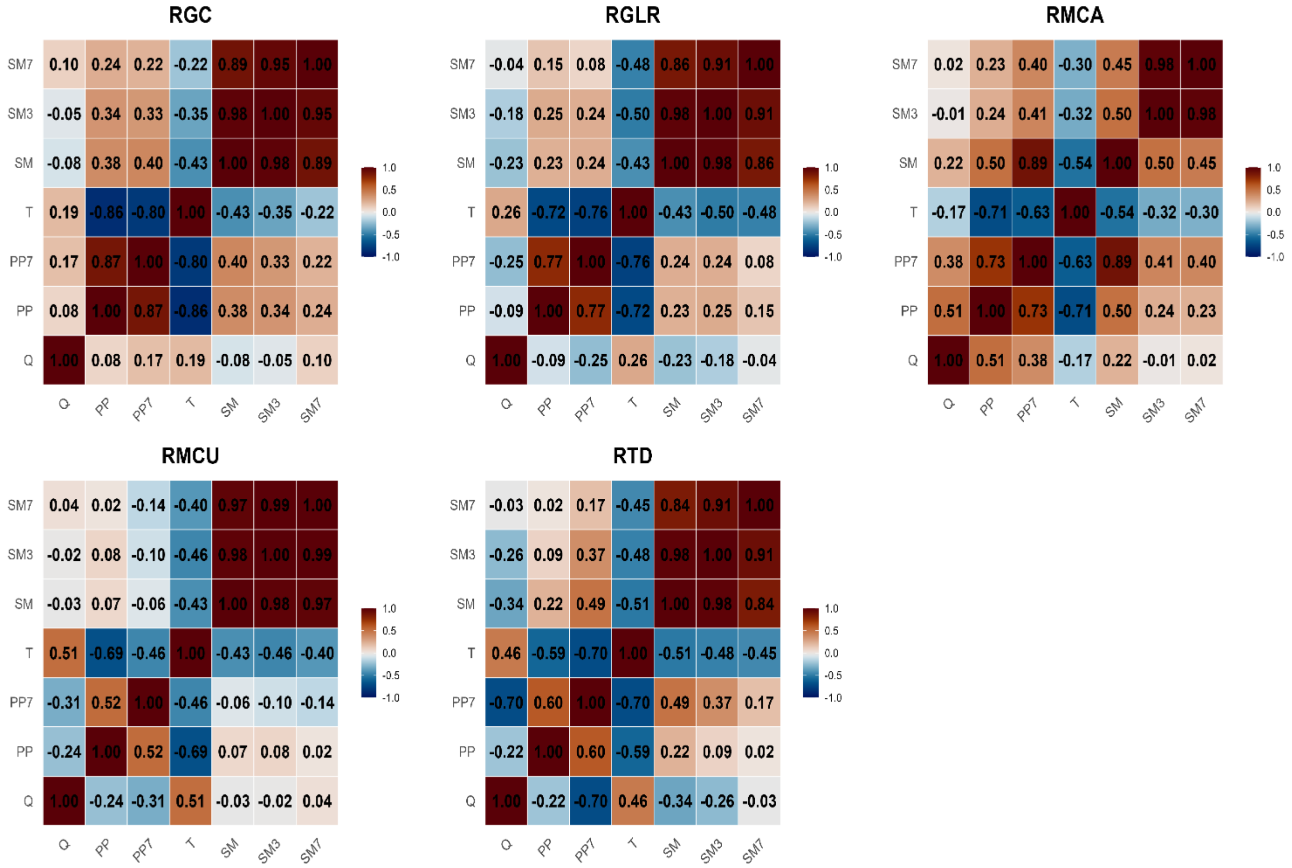

RGC

	Q	PP	PP7	T	SM	SM3	SM7
SM7	0.10	0.24	0.22	-0.22	0.89	0.95	1.00
SM3	-0.05	0.34	0.33	-0.35	0.98	1.00	0.95
SM	-0.08	0.38	0.40	-0.43	1.00	0.98	0.89
T	0.19	-0.86	-0.80	1.00	-0.43	-0.35	-0.22
PP7	0.17	0.87	1.00	-0.80	0.40	0.33	0.22
PP	0.08	1.00	0.87	-0.86	0.38	0.34	0.24
Q	1.00	0.08	0.17	0.19	-0.08	-0.05	0.10

RGLR

	Q	PP	PP7	T	SM	SM3	SM7
SM7	-0.04	0.15	0.08	-0.48	0.86	0.91	1.00
SM3	-0.18	0.25	0.24	-0.50	0.98	1.00	0.91
SM	-0.23	0.23	0.24	-0.43	1.00	0.98	0.86
T	0.26	-0.72	-0.76	1.00	-0.43	-0.50	-0.48
PP7	-0.25	0.77	1.00	-0.76	0.24	0.24	0.08
PP	-0.09	1.00	0.77	-0.72	0.23	0.25	0.15
Q	1.00	-0.09	-0.25	0.26	-0.23	-0.18	-0.04

RMCA

	Q	PP	PP7	T	SM	SM3	SM7
SM7	0.02	0.23	0.40	-0.30	0.45	0.98	1.00
SM3	-0.01	0.24	0.41	-0.32	0.50	1.00	0.98
SM	0.22	0.50	0.89	-0.54	1.00	0.50	0.45
T	-0.17	-0.71	-0.63	1.00	-0.54	-0.32	-0.30
PP7	0.38	0.73	1.00	-0.63	0.89	0.41	0.40
PP	0.51	1.00	0.73	-0.71	0.50	0.24	0.23
Q	1.00	0.51	0.38	-0.17	0.22	-0.01	0.02

RMCU

	Q	PP	PP7	T	SM	SM3	SM7
SM7	0.04	0.02	-0.14	-0.40	0.97	0.99	1.00
SM3	-0.02	0.08	-0.10	-0.46	0.98	1.00	0.99
SM	-0.03	0.07	-0.06	-0.43	1.00	0.98	0.97
T	0.51	-0.69	-0.46	1.00	-0.43	-0.46	-0.40
PP7	-0.31	0.52	1.00	-0.46	-0.06	-0.10	-0.14
PP	-0.24	1.00	0.52	-0.69	0.07	0.08	0.02
Q	1.00	-0.24	-0.31	0.51	-0.03	-0.02	0.04

RTD

	Q	PP	PP7	T	SM	SM3	SM7
SM7	-0.03	0.02	0.17	-0.45	0.84	0.91	1.00
SM3	-0.26	0.09	0.37	-0.48	0.98	1.00	0.91
SM	-0.34	0.22	0.49	-0.51	1.00	0.98	0.84
T	0.46	-0.59	-0.70	1.00	-0.51	-0.48	-0.45
PP7	-0.70	0.60	1.00	-0.70	0.49	0.37	0.17
PP	-0.22	1.00	0.60	-0.59	0.22	0.09	0.02
Q	1.00	-0.22	-0.70	0.46	-0.34	-0.26	-0.03

Figure 8. "BSk(s)-ET(s)" correlation matrices for all combinations of variables.

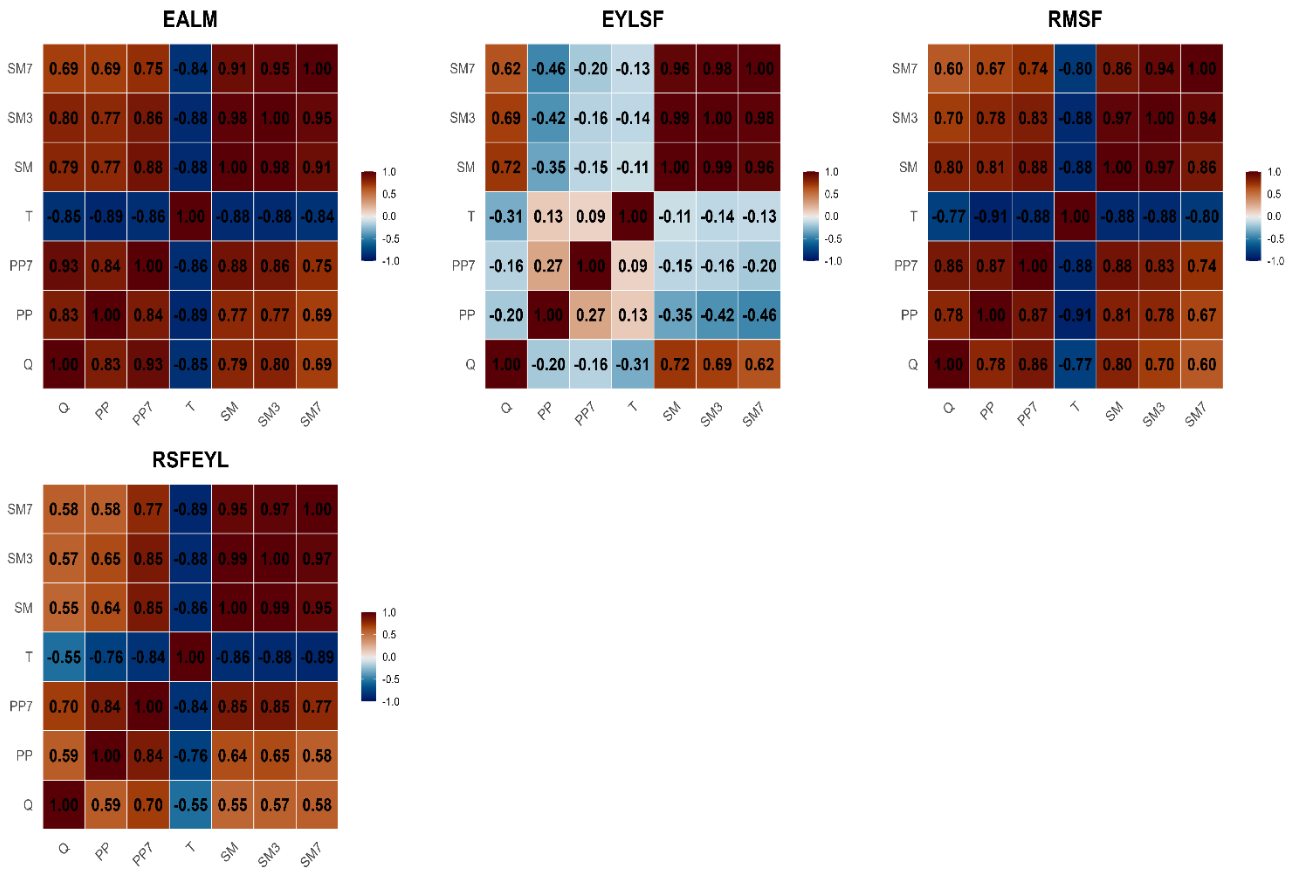

EALM

	Q	PP	PP7	T	SM	SM3	SM7
SM7	0.69	0.69	0.75	-0.84	0.91	0.95	1.00
SM3	0.80	0.77	0.86	-0.88	0.98	1.00	0.95
SM	0.79	0.77	0.88	-0.88	1.00	0.98	0.91
T	-0.85	-0.89	-0.86	1.00	-0.88	-0.88	-0.84
PP7	0.93	0.84	1.00	-0.86	0.88	0.86	0.75
PP	0.83	1.00	0.84	-0.89	0.77	0.77	0.69
Q	1.00	0.83	0.93	-0.85	0.79	0.80	0.69

EYLSF

	Q	PP	PP7	T	SM	SM3	SM7
SM7	0.62	-0.46	-0.20	-0.13	0.96	0.98	1.00
SM3	0.69	-0.42	-0.16	-0.14	0.99	1.00	0.98
SM	0.72	-0.35	-0.15	-0.11	1.00	0.99	0.96
T	-0.31	0.13	0.09	1.00	-0.11	-0.14	-0.13
PP7	-0.16	0.27	1.00	0.09	-0.15	-0.16	-0.20
PP	-0.20	1.00	0.27	0.13	-0.35	-0.42	-0.46
Q	1.00	-0.20	-0.16	-0.31	0.72	0.69	0.62

RMSF

	Q	PP	PP7	T	SM	SM3	SM7
SM7	0.60	0.67	0.74	-0.80	0.86	0.94	1.00
SM3	0.70	0.78	0.83	-0.88	0.97	1.00	0.94
SM	0.80	0.81	0.88	-0.88	1.00	0.97	0.86
T	-0.77	-0.91	-0.88	1.00	-0.88	-0.88	-0.80
PP7	0.86	0.87	1.00	-0.88	0.88	0.83	0.74
PP	0.78	1.00	0.87	-0.91	0.81	0.78	0.67
Q	1.00	0.78	0.86	-0.77	0.80	0.70	0.60

RSFEYL

	Q	PP	PP7	T	SM	SM3	SM7
SM7	0.58	0.58	0.77	-0.89	0.95	0.97	1.00
SM3	0.57	0.65	0.85	-0.88	0.99	1.00	0.97
SM	0.55	0.64	0.85	-0.86	1.00	0.99	0.95
T	-0.55	-0.76	-0.84	1.00	-0.86	-0.88	-0.89
PP7	0.70	0.84	1.00	-0.84	0.85	0.85	0.77
PP	0.59	1.00	0.84	-0.76	0.64	0.65	0.58
Q	1.00	0.59	0.70	-0.55	0.55	0.57	0.58

Figure 9. "ET(s)-Csb(h)-Csc" correlation matrices for all combinations of variables.

In high-altitude transitional climates (ET(s)–Csb(h)–Csc; Fig. 9), temperature exhibits strong negative correlations with streamflow, precipitation and soil moisture, indicating that warmer conditions are associated with drier antecedent states. Despite this, streamflow remains positively associated with precipitation and soil moisture, suggesting that peak flows are primarily controlled by water availability, while temperature modulates antecedent conditions rather than directly driving runoff generation.

In contrast, the BSk(s)–ET(s) zone (Fig. 8) displays a markedly different behaviour. Here, correlations between streamflow and precipitation are weak or even negative, indicating that peak flows are not directly associated with precipitation occurring on the same day. Similarly, relationships between streamflow and soil moisture are weak and inconsistent. This pattern suggests that peak flows in this region are influenced by delayed processes, rather than by immediate hydroclimatic conditions at the event date.

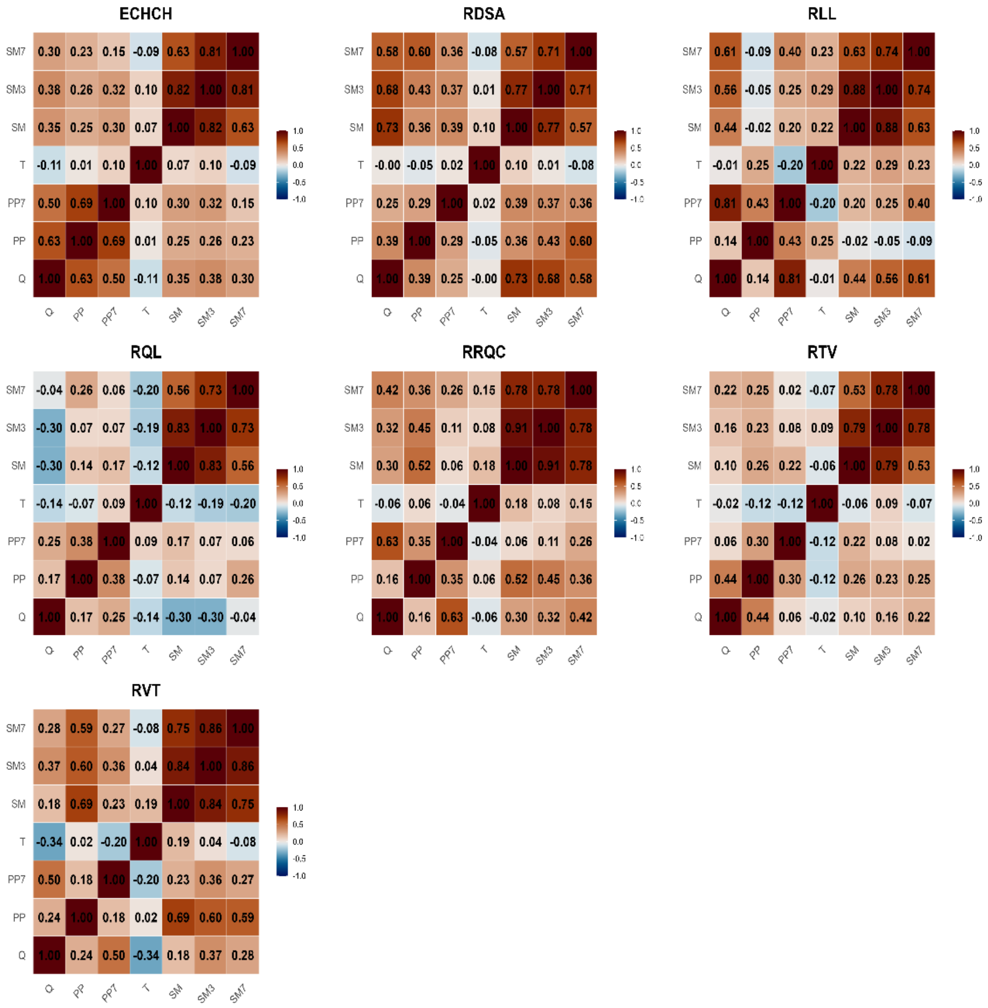

ECHCH

	Q	PP	PP7	T	SM	SM3	SM7
SM7	0.30	0.23	0.15	-0.09	0.63	0.81	1.00
SM3	0.38	0.26	0.32	0.10	0.82	1.00	0.81
SM	0.35	0.25	0.30	0.07	1.00	0.82	0.63
T	-0.11	0.01	0.10	1.00	0.07	0.10	-0.09
PP7	0.50	0.69	1.00	0.10	0.30	0.32	0.15
PP	0.63	1.00	0.69	0.01	0.25	0.26	0.23
Q	1.00	0.63	0.50	-0.11	0.35	0.38	0.30

RDSA

	Q	PP	PP7	T	SM	SM3	SM7
SM7	0.58	0.60	0.36	-0.08	0.57	0.71	1.00
SM3	0.68	0.43	0.37	0.01	0.77	1.00	0.71
SM	0.73	0.36	0.39	0.10	1.00	0.77	0.57
T	-0.00	-0.05	0.02	1.00	0.10	0.01	-0.08
PP7	0.25	0.29	1.00	0.02	0.39	0.37	0.36
PP	0.39	1.00	0.29	-0.05	0.36	0.43	0.60
Q	1.00	0.39	0.25	-0.00	0.73	0.68	0.58

RLL

	Q	PP	PP7	T	SM	SM3	SM7
SM7	0.61	-0.09	0.40	0.23	0.63	0.74	1.00
SM3	0.56	-0.05	0.25	0.29	0.88	1.00	0.74
SM	0.44	-0.02	0.20	0.22	1.00	0.88	0.63
T	-0.01	0.25	-0.20	1.00	0.22	0.29	0.23
PP7	0.81	0.43	1.00	-0.20	0.20	0.25	0.40
PP	0.14	1.00	0.43	0.25	-0.02	-0.05	-0.09
Q	1.00	0.14	0.81	-0.01	0.44	0.56	0.61

RQL

	Q	PP	PP7	T	SM	SM3	SM7
SM7	-0.04	0.26	0.06	-0.20	0.56	0.73	1.00
SM3	-0.30	0.07	0.07	-0.19	0.83	1.00	0.73
SM	-0.30	0.14	0.17	-0.12	1.00	0.83	0.56
T	-0.14	-0.07	0.09	1.00	-0.12	-0.19	-0.20
PP7	0.25	0.38	1.00	0.09	0.17	0.07	0.06
PP	0.17	1.00	0.38	-0.07	0.14	0.07	0.26
Q	1.00	0.17	0.25	-0.14	-0.30	-0.30	-0.04

RRQC

	Q	PP	PP7	T	SM	SM3	SM7
SM7	0.42	0.36	0.26	0.15	0.78	0.78	1.00
SM3	0.32	0.45	0.11	0.08	0.91	1.00	0.78
SM	0.30	0.52	0.06	0.18	1.00	0.91	0.78
T	-0.06	0.06	-0.04	1.00	0.18	0.08	0.15
PP7	0.63	0.35	1.00	-0.04	0.06	0.11	0.26
PP	0.16	1.00	0.35	0.06	0.52	0.45	0.36
Q	1.00	0.16	0.63	-0.06	0.30	0.32	0.42

RTV

	Q	PP	PP7	T	SM	SM3	SM7
SM7	0.22	0.25	0.02	-0.07	0.53	0.78	1.00
SM3	0.16	0.23	0.08	0.09	0.79	1.00	0.78
SM	0.10	0.26	0.22	-0.06	1.00	0.79	0.53
T	-0.02	-0.12	-0.12	1.00	-0.06	0.09	-0.07
PP7	0.06	0.30	1.00	-0.12	0.22	0.08	0.02
PP	0.44	1.00	0.30	-0.12	0.26	0.23	0.25
Q	1.00	0.44	0.06	-0.02	0.10	0.16	0.22

RVT

	Q	PP	PP7	T	SM	SM3	SM7
SM7	0.28	0.59	0.27	-0.08	0.75	0.86	1.00
SM3	0.37	0.60	0.36	0.04	0.84	1.00	0.86
SM	0.18	0.69	0.23	0.19	1.00	0.84	0.75
T	-0.34	0.02	-0.20	1.00	0.19	0.04	-0.08
PP7	0.50	0.18	1.00	-0.20	0.23	0.36	0.27
PP	0.24	1.00	0.18	0.02	0.69	0.60	0.59
Q	1.00	0.24	0.50	-0.34	0.18	0.37	0.28

Figure 10. "Csb" correlation matrices for all combinations of variables.

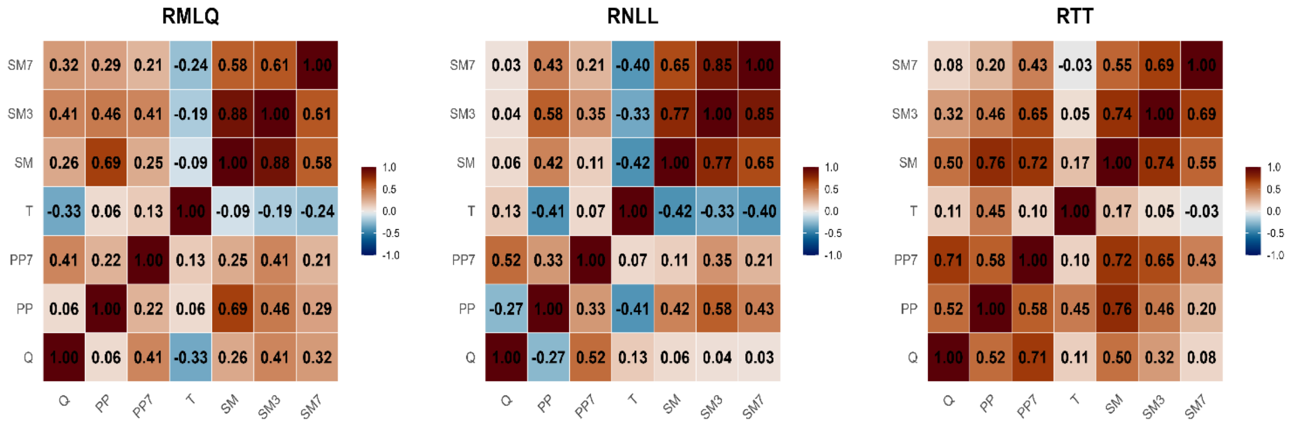

RMLQ

	Q	PP	PP7	T	SM	SM3	SM7
SM7	0.32	0.29	0.21	-0.24	0.58	0.61	1.00
SM3	0.41	0.46	0.41	-0.19	0.88	1.00	0.61
SM	0.26	0.69	0.25	-0.09	1.00	0.88	0.58
T	-0.33	0.06	0.13	1.00	-0.09	-0.19	-0.24
PP7	0.41	0.22	1.00	0.13	0.25	0.41	0.21
PP	0.06	1.00	0.22	0.06	0.69	0.46	0.29
Q	1.00	0.06	0.41	-0.33	0.26	0.41	0.32

RNLL

	Q	PP	PP7	T	SM	SM3	SM7
SM7	0.03	0.43	0.21	-0.40	0.65	0.85	1.00
SM3	0.04	0.58	0.35	-0.33	0.77	1.00	0.85
SM	0.06	0.42	0.11	-0.42	1.00	0.77	0.65
T	0.13	-0.41	0.07	1.00	-0.42	-0.33	-0.40
PP7	0.52	0.33	1.00	0.07	0.11	0.35	0.21
PP	-0.27	1.00	0.33	-0.41	0.42	0.58	0.43
Q	1.00	-0.27	0.52	0.13	0.06	0.04	0.03

RTT

	Q	PP	PP7	T	SM	SM3	SM7
SM7	0.08	0.20	0.43	-0.03	0.55	0.69	1.00
SM3	0.32	0.46	0.65	0.05	0.74	1.00	0.69
SM	0.50	0.76	0.72	0.17	1.00	0.74	0.55
T	0.11	0.45	0.10	1.00	0.17	0.05	-0.03
PP7	0.71	0.58	1.00	0.10	0.72	0.65	0.43
PP	0.52	1.00	0.58	0.45	0.76	0.46	0.20
Q	1.00	0.52	0.71	0.11	0.50	0.32	0.08

Figure 11. "Cfb(i)‑Cfb" correlation matrices for all combinations of variables.

In Mediterranean and temperate climates (Csb and Cfb(i)–Cfb; Fig. 10–11), streamflow is positively associated with both precipitation and soil moisture. The relationship is generally stronger for accumulated precipitation (PP7), highlighting the importance of multi-day rainfall events. Soil moisture variables also show consistent positive correlations with streamflow, indicating the role of antecedent wetness conditions in modulating runoff response. In contrast, temperature exhibits weak and spatially variable correlations with the other variables, suggesting a limited direct influence on peak flow conditions.

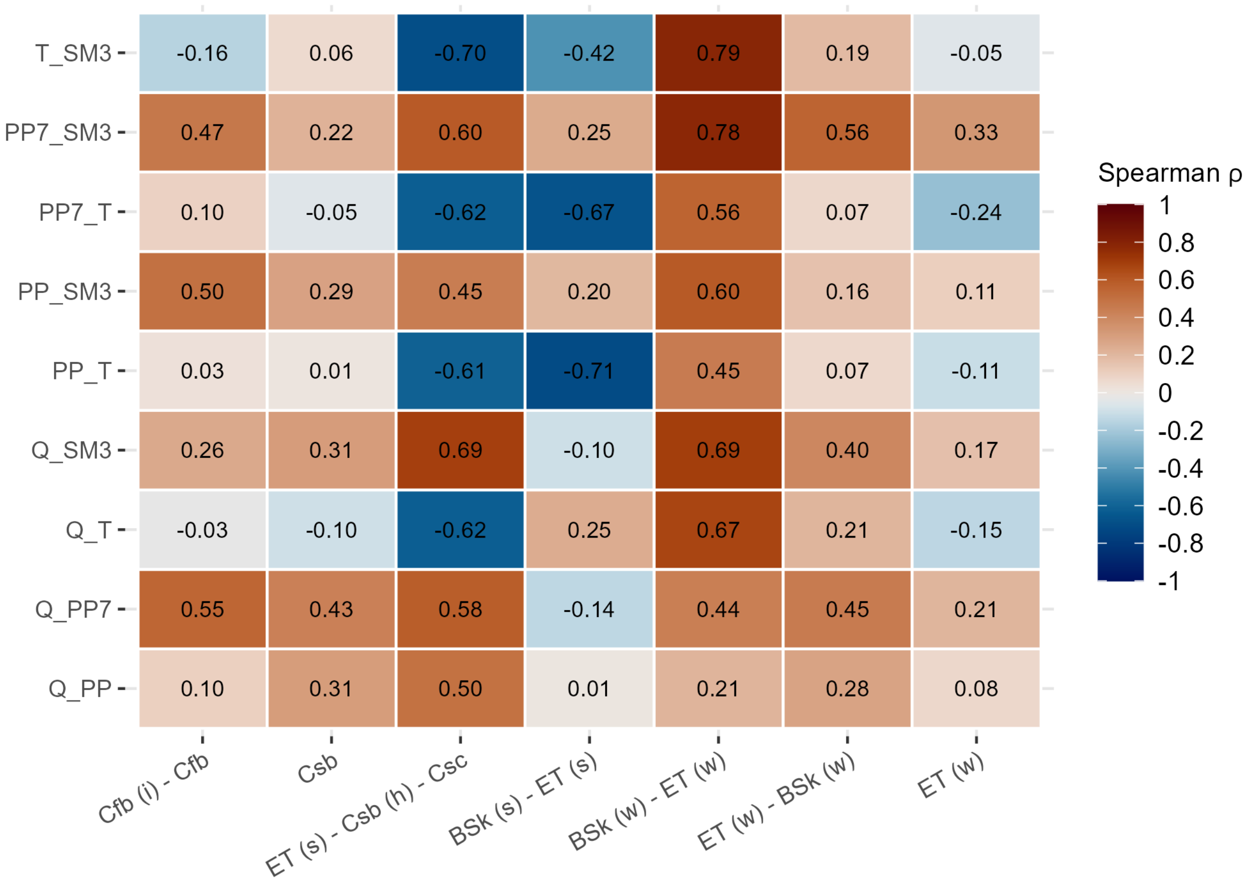

Figure 1. Synthetic heatmap of average correlations across climatic zones. In the Y axis are the correlations between two maximum variables.

The synthetic heatmap (Fig. 12) summarizes the median correlations across climate zones and reinforces three key patterns: (i) the consistent role of accumulated precipitation in shaping peak flows, (ii) the strong coupling between precipitation and soil moisture, particularly under sustained wet conditions, and (iii) the increasing influence of temperature in high-altitude and water-limited environments.

4 Discussion

4.1 Trends

Within individual climate zones, some catchments exhibit differences in the direction or significance of trends. This intra-zone variability reflects the influence of local catchment characteristics and hydroclimatic conditions, which can modulate the response of streamflow to climatic forcing. Therefore, while climate zones provide a useful regional framework for comparison, they do not imply uniform hydrological behaviour across all catchments. These differences highlight the importance of interpreting regional patterns alongside local variability, rather than assuming homogeneous responses within each climate group.

The proportion of annual maximum streamflow values associated with gap-filled data was quantified to assess the potential influence of reconstructed observations on the analysis. After excluding stations located in artificial channels or clearly affected by flow regulation, 103 out of 638 annual maxima (16.1%) corresponded to infilled values. This indicates that most annual maxima used in the analysis were derived from observed records, although reconstructed data still represent a non-negligible fraction of the dataset.

Streamflow trends show a general tendency towards decreasing values across mediterranean (Csb and ET(s)–Csb(h)–Csc), temperate (Cfb(i)–Cfb) and winter-rainfall (BSk(s)–ET(s), Csb and ET(s)–Csb(h)–Csc) climate zones. This pattern is consistent with previous findings highlighting the importance of winter precipitation in these regions (Blöschl et al., 2019), although variability exists among individual catchments. These declines are likely driven by reduced winter rainfall and enhanced evapotranspiration under warmer conditions, linked to the megadrought and the broader global pattern affecting winter-rainfall regions (IPCC 2023). Semi-arid areas exhibit a more heterogeneous but predominantly negative behaviour, consistent with observations in arid and warm-dry regions of North America and Australia (Do et al., 2017) and in northeastern Iran (Minaei and Irannezhad, 2018). This contrast between semi-arid winter-rainfall and summer-rainfall climates highlights that streamflow dependence on precipitation is stronger in the former. In contrast, local and coastal influences modulate or attenuate trends in the latter.

Precipitation also shows mainly negative trends, particularly in mediterranean and temperate zones (CSb, ET(s)–Csb(h)–Csc and Cfb(i)–Cfb), which become more evident when considering seven-day accumulated precipitation, including ocean-moderated regions. Similar declines have been reported for central and southern Chile (Oertel et al., 2020; Sangüesa et al., 2023; Stolpe et al., 2016). These findings suggest that winter precipitation plays an important role in shaping annual maximum streamflow (Q) in mediterranean (Csb and ET(s)–Csb(h)–Csc) and temperate (Cfb(i)–Cfb) regions, in contrast to the weaker or non-significant changes observed in tundra and summer-rainfall climates.

Global warming intensifies these effects, especially in drier catchments. While Vicuña et al. (2013) proposed that extreme heat might increase the contributing runoff area. Temperature increases across all climates, particularly coastal temperate catchments, further reinforce the drying signal.

Soil moisture trends exhibit contrasting behaviour across climatic zones, reflecting the combined influence of precipitation regimes and temperature. In winter-rainfall climates – particularly Mediterranean and temperate regions (CSb, ET(s)–Csb(h)–Csc and Cfb(i)–Cfb) – soil moisture shows predominantly negative trends, consistent with the joint effects of declining precipitation and increasing temperature, which reduce soil water availability and limit recharge. The increasingly negative trends from SM to SM3 and SM7 indicate cumulative water deficits and reduced soil recovery between rainfall events, which, in turn, contribute to the observed declines in streamflow. In contrast, summer-rainfall climates (ET(w)–BSk(w), BSk(w)–ET(w) and ET(w)) display mostly stable soil moisture trends, especially in semi-arid catchments where convective summer storms sustain short-term replenishment despite high temperatures. Coastal temperate catchments, influenced by oceanic humidity, exhibit milder declines, confirming that maritime moderation partially offsets the drying signal. This underscores the need to integrate physical variables, not just meteorological ones, to understand mechanisms of hydrological change.

These consistent patterns suggest that the hydro-climatic behaviour observed in Chile can be extended to other regions with comparable climatic settings. Mediterranean and winter-rainfall climates worldwide appear to share a drying trajectory, driven by declining precipitation, as documented in southern Europe (Yeste et al., 2018; Gentilucci and Hamed, 2023; Myronidis et al., 2018) and parts of Australia and North America (Do et al., 2018). Semi-arid climates exhibit greater spatial heterogeneity, yet the predominance of negative streamflow trends suggests similar vulnerabilities to warming and increased evapotranspiration. Conversely, tundra and summer-rainfall climates exhibit weaker or mixed signals, confirming that snowmelt-dominated and convective systems respond differently to climate forcing. Recognising these consistent responses across climate types is crucial, as it allows extending hydrological inferences to regions with limited observations and supports the development of climate-specific strategies for assessing and managing water resources under global warming.

4.2 Correlations

The analyzed catchments span a wide range of hydroclimatic conditions across Chile, including rainfall-dominated systems as well as catchments where snow processes may contribute to streamflow generation. The interpretation of the results indicates that differences in the strength of the relationships between hydroclimatic variables and peak streamflow are consistent with variations in dominant runoff-generation processes across regions. For example, in rainfall-dominated catchments, stronger associations with precipitation are expected, whereas in catchments with snow influence or greater spatial heterogeneity, these relationships may be weaker or more diffuse due to storage and delayed release processes.

Correlations indicate that precipitation, particularly multi-day accumulation, is strongly associated with annual maximum streamflow and soil moisture within the study catchments, consistent with previous findings (Blöschl et al., 2019). These relationships are stronger in winter-rainfall climates (BSk(s)–ET(s), CSb, ET(s)–Csb(h)–Csc and Cfb(i)–Cfb), where prolonged rainfall events govern runoff generation. Streamflow in some tundra climates (ET(w), BSk(s)-ET(s) and ET(s)-Csb(h)-Csc), however, correlates more closely with temperature than precipitation. Specifically, in mediterranean climate (Csb, Csc), we can see a strong precipitation control, declining trends in all hydroclimatic variables. In the case of temperate oceanic climate (Cfb, Cfc), there is a strong precipitation-streamflow correlation, moderate declining trends, and soil moisture acts as an important intermediate control. For the Cold semi-arid climate (BSk), a weaker precipitation-streamflow coupling, high interannual variability, and pronounced temperature effects are observed. In the tundra climate (ET), we encountered mixed streamflow trends, a strong warming signal.

Analyzing the different variables, behaviour temperature generally shows weak and inverse correlations, but exerts a stronger influence in tundra and semi-arid climates and in transition zones (BSk(s)–ET(s), ET(w)–BSk(w), BSk(w)–ET(w), ET(w), CSb and ET(s)–Csb(h)–Csc). Rising temperatures enhance evapotranspiration, reduce snowmelt contributions, and alter soil moisture patterns, consistent with observations in Spain (Yeste et al., 2018) and Cyprus (Myronidis et al., 2018). Soil moisture–streamflow correlations are more evident when using smoothed soil moisture indices, which better reflect storage capacity. In mediterranean and temperate zones (CSb, ET(s)–Csb(h)–Csc and Cfb(i)–Cfb), this relationship is direct, indicating that greater soil retention limits the immediate runoff response. In contrast, Wasko and Nathan (2019) found the opposite pattern in Australia, where soil moisture better explains streamflow variability when rainfall dependence is low. Here, only tundra climates showed no significant soil moisture–streamflow link, whereas semi-arid regions did, helping clarify previous uncertainty noted by Sangüesa et al. (2023).

In summary, accumulated precipitation shows a strong association with annual maximum streamflow in mediterranean (Csb and ET(s)–Csb(h)–Csc), temperate (Cfb(i)–Cfb) and winter-rainfall (BSk(s)–ET(s), Csb and ET(s)–Csb(h)–Csc) climates. Soil moisture is also associated with variations in streamflow, suggesting a potential role in modulating runoff responses, while temperature exhibits contrasting relationships across climate zones. Altogether, these patterns are consistent with a general tendency towards decreasing streamflow in winter-rainfall (BSk(s)–ET(s), Csb and ET(s)–Csb(h)–Csc) regions, in conjunction with concurrent changes in precipitation and temperature observed in these catchments. These results reflect statistical associations identified within the study dataset and should be interpreted within the limitations of the analysis.

These relationships are consistent with hydro-climatic dynamics observed in comparable regions worldwide. In mediterranean and temperate climates (CSb, ET(s)–Csb(h)–Csc and Cfb(i)–Cfb), the strong dependence of streamflow on accumulated precipitation reflects the dominance of frontal winter systems, similar to patterns reported for southern Europe and Australia (Blöschl et al., 2019; Wasko and Nathan, 2019). In contrast, the weaker, more temperature-driven relationships in tundra and semi-arid climates (BSk(s)–ET(s), ET(w)–BSk(w), BSk(w)–ET(w) and ET(w)) mirror those of snow- and heat-controlled basins in Asia and North America, where evapotranspiration and melt processes dominate runoff generation. This suggests that the coupling between precipitation, soil moisture, and streamflow observed in Chile can be extended to analogous climates globally, providing a framework for anticipating hydrological behaviour in data-scarce regions.

A limitation of this study is the relatively short record length (2000–2021), which may affect the robustness of trend detection, particularly for annual maxima that are inherently characterized by high interannual variability. Short time series can reduce the statistical power of trend tests and increase the sensitivity of results to individual extreme events.

However, the objective of this study is not to infer long-term historical trends, but rather to characterize recent hydroclimatic tendencies under current climate conditions. In this context, the selected period captures a climatically relevant interval that includes significant recent variability in Chile, including the megadrought (2010–2020), providing meaningful insight into contemporary streamflow behaviour.

Land use and land cover changes, such as forest plantations and urban expansion in Chile (Miranda et al., 2017), were not explicitly accounted for but may influence streamflow independently of climate. The coarse spatial resolution of gridded climate datasets (e.g., CR2MET) and satellite soil moisture products introduces uncertainty, particularly in mountainous areas where orographic effects and steep terrain affect data accuracy (Garreaud, 2009; Al-Yaari et al., 2019).